Simultaneous multiphase flash and stability analysis calculations including solid CO_2 for CO_2-CH_4, CO_2-CH_4-N_2 and CO_2-CH_4-N_2-O_2 mixtures

Giorgia De Guido[a,*], *Elvira Spatolisano*[a]

[a]*GASP - Group on Advanced Separation Processes & GAS Processing, Dipartimento di Chimica, Materiali e Ingegneria Chimica "Giulio Natta", Politecnico di Milano, Piazza Leonardo da Vinci 32, I-20133 Milano, Italy*

giorgia.deguido@polimi.it; elvira.spatolisano@polimi.it

[*]*Corresponding author: Giorgia De Guido (giorgia.deguido@polimi.it; phone: +39 02 2399 3260; fax: +39 02 2399 3280; full postal address: Dipartimento di Chimica, Materiali e Ingegneria Chimica "G. Natta", Politecnico di Milano, Piazza Leonardo da Vinci 32, I-20133 Milan, Italy)*

Abstract

This work deals with solid-vapor equilibria and solid-liquid-vapor equilibria of carbon dioxide in mixtures of interest for natural gas purification and biogas upgrading. Experimental data available in the literature are reviewed and an algorithm for solving an isobaric-isothermal flash coupled to a phase stability analysis is presented, which does not require to know *a-priori* the number and type of phases existing at equilibrium. The good agreement between calculation results, also performed with a tool that makes use of Gibbs free energy minimization, and experimental data suggests that the proposed approach can be used for determining suitable operating conditions for processes aimed at separating CO_2 out of the gas by freezing it.

This work points out that more experimental studies should be performed on phase equilibria in the presence of solid CO_2 for multicomponent mixtures containing species other than methane (e.g., nitrogen and oxygen), which are representative of gaseous streams from which CO_2 needs to be removed, such as natural gas, biogas, and flue gas from power plants. Such data are important for a proper calibration of thermodynamic models that have to be selected for reliable process simulations.

Keywords: carbon dioxide, solid-vapor equilibria, solid-liquid-vapor equilibria, experimental data, thermodynamic modeling

1. Introduction

In the process industry field, one of the biggest concerns has always been the sweetening of acid gaseous streams. During the last decades, various technologies have been studied and tested in order to efficiently reduce the amount of acid components in these streams. In particular, the attention has been focused on the carbon dioxide removal. In fact, CO_2 is considered as one of the most significant greenhouse gases, and its increasing concentration in the atmosphere plays a major role in increasing global warming. Moreover, the presence of high CO_2 contents in natural gas results in a reduction of the calorific value and causes corrosion of the pipeline and equipment, along with many other operational problems.[1] Among the established CO_2 separation strategies, recently CO_2 capture using low-temperature/cryogenic technologies has received increasing attention. Previous works have demonstrated they have lower energy consumptions than conventional amine scrubbing both if applied to natural gas purification[2] and to biogas upgrading.[3] Another advantage they offer is that pure CO_2 is separated as a liquid under pressure rather than in the gaseous state at near ambient pressure, thus making it relatively easy to pump underground for storage or to be used for Enhanced Oil Recovery (EOR) applications.[4]

This has boosted an intense research activity on measurement and thermodynamic modeling of CO_2 frost points and other types of phase equilibria involving solid CO_2 in natural gas or biogas mixtures. Both activities are important to correctly describe the thermodynamic behavior of the system of interest, which in turn plays a key role in the design of novel low-temperature/cryogenic processes.

The aim of this work is twofold. First of all, it focuses on the solid-vapor equilibrium (SVE) and solid-liquid-vapor equilibrium (SLVE) experimental data available in the literature for systems containing CO_2 and methane, nitrogen and oxygen. In section 2, for each dataset, the following information is reported (when available): the experimental procedure, the mixture composition or the range of CO_2 concentrations, the temperature and pressure range and the number of points. Then, in section 3, an algorithm is presented for the simultaneous computation of phase stability and multiphase equilibria of CO_2-containing mixtures. Section 4 presents the results of the calculations, which are also compared with those given by another tool that makes use of Gibbs free energy minimization.

2. Experimental data

This section deals with the available literature concerning phase equilibria in the presence of solid CO_2, focusing on CO_2-CH_4 mixtures and on ternary and quaternary mixtures that also contain N_2 and O_2. The latter systems are of interest considering that nitrogen is a classical natural gas impurity[5] and, in some cases, air is present in the raw biogas (e.g., in biogas produced in landfills).

Data for the temperature and pressure are reported in Kelvin and in bar, respectively. Therefore, the data available in the literature have been converted when reported in different units of measurement. The global composition of the analyzed mixtures is also reported, when available.

2.1 The CO_2-CH_4 system

Table 1 summarizes the SVE data available in the literature for the CO_2-CH_4 system, which are organized on the basis of their literature source. Detailed data are reported in Tables S1-S6 in the *Supporting Information*.

In his Ph.D. thesis work, Pikaar[6] determined the phase equilibria of the CO_2-CH_4 system using two methods. A non-sampling technique was used to determine frost points of mixtures with a CO_2 content ranging from 1 to 20 mol.%, while a sampling method was used to determine the composition of the vapor phase in equilibrium with solid CO_2 at temperatures from 133.15 to 210.15 K. Le and Trebble[7] observed there exist slight variances in Pikaar's two datasets, especially at lower CO_2 concentrations.

Agrawal and Laverman[8] used a non-sampling visual technique in which a known gas mixture of CO_2-CH_4 was charged into the cell (i.e., the cryostat), and the pressure and temperature at which the solid phase just began to form were determined. Their data included frost point measurements for five different binary mixtures of CO_2 and CH_4 containing, respectively: 0.12 mol.% CO_2, 0.97 mol.% CO_2, 1.8 mol.% CO_2, 3.07 mol.% CO_2, 10.67 mol.% CO_2.

Le and Trebble[7] pointed out there is considerable disagreement at higher pressures (at which natural gas processing plants are usually operated) for the SVE data presented in the years before in the above-mentioned literature works. In an attempt to reconcile these differences, they used a non-sampling technique to perform frost point measurements on three different CO_2-CH_4 mixtures containing, respectively, 1.00 mol.% CO_2, 1.91 mol.% CO_2, 2.93 mol.% CO_2 at 9.621 to 30.082 bar and 168.6 to 187.7 K.

Some years later, Zhang and co-workers[9] presented new experimental data for the frost points of CO_2-CH_4 mixtures covering a wide range of CO_2 concentrations, from 10.8 to 54.2 mol.% CO_2. Thus, they extended the analysis performed in previous years to systems of interest when considering the removal of CO_2 from high carbon dioxide-content natural gas fields, which is important to the gas industry development in some countries (e.g., Indonesia and Malaysia).[10]

The work by Xiong et al.[11] provides CO_2 SVE data over a wide range of composition, temperature, and pressure in the region of practical application for the natural gas industry. The method to collect phase equilibrium data was the static analytic method with sampling technique, so providing the composition of the vapor phase at equilibrium.

Table 1. SVE experimental data available in the literature for the CO_2-CH_4 system.

Literature source	Measurement technique	Data type	Mixture	*T* [K]	*P* [bar]	No. points
Pikaar (1959)[6]	Non-sampling technique	Frost points (*T*, *P*)	1 to 20 mol.% CO_2	158.25 to 210.48	1.966 to 48.322	38
	Sampling technique	*P*, $x_{CO2,V}$ at 7 temperatures	Not available[a]	133.15 to 210.15	1.56 to 47.896	66
Agrawal and Laverman (1995)[8]	Non-sampling visual technique	Frost points (*T*, *P*) for 5 mixtures	0.12 to 10.67 mol.% CO_2	137.54 to 198.09	1.724 to 27.855	42
Le and Trebble (2007)[7]	Non-sampling visual technique	Frost points (*T*, *P*) for 3 mixtures	1.00 to 2.93 mol.% CO_2	168.6 to 187.7	9.621 to 30.082	55
Zhang et al. (2011)[9]	Isochoric method	Frost points (*T*, *P*) for 5 mixtures	10.8 to 54.2 mol.% CO_2	191.1 to 210.3	2.93 to 44.46	17
Xiong et al. (2015)[11]	Static analytic method with sampling technique	SVE (*T, P,* $x_{CO2,V}$) at 6 temperatures	0.5 to 20.1 mol.% CO_2	153.15 to 193.15	2.19 to 30.38	64

[a] The global composition of the mixture for which solid-vapor equilibrium conditions were determined experimentally by Pikaar[6] using the saturation cell apparatus is not given in his PhD thesis, where it is reported that at the beginning of the experiment the walls of the saturation cell were coated with solid CO_2 and this solid saturated the methane flowing through the cell from the storage.

Table 2 summarizes the SLVE data available in the literature for the CO_2-CH_4 mixture, which is well known to exhibit a SLVE locus that passes through a maximum in the *P vs. T* diagram. Detailed data are reported in Tables S7-S14 in the *Supporting Information*. In Table 2, the data from Shen et al.[12] and Gao et al.[13] are not considered, since they are presented as SLE data, though Riva and Stringari[14] observed they are actually SLVE data for which only the CO_2 mole fraction in the liquid phase was reported.

Donnelly and Katz[15] presented data in terms of temperature and pressure pairs along the SLVE locus. In addition to that, they also showed two isobaric temperature-composition diagrams (at 500 and 673 psia, respectively, as shown in Figure S1 in the *Supporting Information*), which can be used to obtain other four *T*, *P* conditions where SLVE establishes for the system CO_2-CH_4.

The experimental work by Sterner[16] was undertaken as a result of the need to extend the work done by Donnelly and Katz[15] to low temperatures. The data presented are of particular interest because they differ considerably from some of the results presented by Donnelly and Katz,[15] especially their extrapolation of SLVE points to lower temperatures.

The experimental work by Davis and co-workers[17] was carried out to determine the SLV phase behavior of the CO_2-CH_4 mixture at CO_2 concentrations commonly encountered in natural gas.

Im and Kurata[18] summarized the data reported by Davis et al.[17] and Brewer and Kurata[19] concerning the SLV locus of the CO_2-CH_4 system.

Table 2: SLVE experimental data available in the literature for the CO_2-CH_4 system.

Literature source	Data type	*T* [K]	*P* [bar]	No. points
Donnelly and Katz (1954)[15]	*T, P*	191.76 to 215.65	9.170 to 48.539	25[a]
Sterner (1961)[16]	*T, P*	166.43 to 199.93	19.472 to 49.887	6[b]
	T-$x_{CO2,V}$	166.5 to 202.4	19.305 to 49.987	8[c]
	T-$x_{CO2,L}$	166.9 to 177.7	19.305 to 28.958	3[c]
Davis et al. (1962)[17]	*T, P*	97.54 to 211.71	0.283 to 48.677	38
	T-$x_{CO2,V}$	140.93 to 205.71	6.895 to 48.263	8[d]
	T-$x_{CO2,L}$	129.65 to 201.26	3.447 to 48.263	11[d]
Im and Kurata (1971)[18]	T-P-$x_{CO2,V}$-$x_{CO2,L}$	165.21 to 210.21	18.961 to 48.470	10

[a] Including the four *T*, *P* conditions that can be read from the two isobaric temperature-composition diagrams (at 500 and 673 psia, respectively, as shown in Figure S1 in the Supporting Information) reported by Donnelly and Katz.[15]

[b] Obtained from the *P vs. T* plot reported by Sterner.[16]

[c] Obtained from the *T*-composition plot reported by Sterner.[16] The pressure ranges reported for these two datasets have been inferred considering the temperature range they refer to and with the aid of the *P vs. T* plot reported by Sterner.[16]

[d] The pressure ranges reported for these two datasets have been inferred considering the temperature range they refer to and with the aid of the *P vs. T* plot reported by Davis et al.[17]

2.2 The CO_2-CH_4-N_2 system

As previously pointed out, since nitrogen may be present in the gaseous streams to be treated for removing CO_2 by low-temperature/cryogenic technologies, it is important to collect phase equilibrium data in the presence of solid CO_2 also for this ternary mixture. Agrawal and Laverman,[8] Le and Trebble,[7] and Xiong et al.[11] performed frost point measurements for this ternary system, whereas SLVE was investigated by Riva and Stringari.[14] Table 3 summarizes the data available in the literature. More details on SVE data are reported in Tables S15-S18 in the *Supporting Information*. In Table 3, the data from Shen et al.[12] and Gao et al.[13] are not reported, since they are presented as SLE data, though Riva and Stringari[14] observed they are actually SLVE data for which only the CO_2 mole fraction in the liquid phase was reported.

Focusing on frost point data first, Agrawal and Laverman[8] performed measurements on two CO_2-CH_4-N_2 mixtures having a composition similar to that of typical natural gases with a low content of CO_2. The authors also reported some frost point data published by Haufe et al.[20] for two mixtures of the three components richer in N_2 (*ca.* 63 mol.%), which are also included in Table 3.

CO_2 frost point data for the CO_2-CH_4-N_2 system were also collected by Le and Trebble[7] for mixtures containing 1 mol.% and 1.95 mol.% N_2.

To investigate the influence of nitrogen on the CO_2 frost points, two types of CO_2-CH_4-N_2 ternary mixtures were investigated by Xiong et al.[11] which contained, respectively, 3 mol.% N_2 and 5 mol.% N_2.

Table 3 also reports SLVE data available in the literature for the CO_2-CH_4-N_2 system: Riva and Stringari[14] examined two different mixtures containing, respectively, 2 mol.% CO_2, 58 mol.% CH_4, 40 mol.% N_2 and 2 mol.% CO_2, 79 mol.% CH_4, 19 mol.% N_2 and reported the measured composition of the liquid and vapor phases at each temperature and pressure. More details on these SLVE data are reported in Tables S19-S20 in the *Supporting Information*.

Table 3. SVE and SLVE experimental data available in the literature for the CO_2-CH_4-N_2 mixture.

Literature source	Measurements technique	Data type	Mixture composition	*T* [K]	*P* [bar]	No. points
			SVE			
Haufe et al. (1972)[20]	Sampling technique	Frost points (*T, P*)	0.21 mol.% CO_2-36.5 mol.% CH_4-63.3 mol.% N_2 0.45 mol.% CO_2-36.5 mol.% CH_4-63.0 mol.% N_2	151.48 to 165.21	10.059 to 39.948	5[a]
Agrawal and Laverman (1995)[8]	Non-sampling visual technique	Frost points (*T, P*)	0.96 mol.% CO_2-98.36 mol.% CH_4-0.68 mol.% N_2 0.93 mol.% CO_2-96.13 mol.% CH_4-2.94 mol.% N_2	154.15 to 172.76	1.724 to 24.407	19
Le and Trebble (2007)[7]	Non-sampling visual technique	Frost points (*T, P*)	1.94 mol.% CO_2-97.06 mol.% CH_4-1 mol.% N_2 1.94 mol.% CO_2-96.11 mol.% CH_4-1.95 mol.% N_2	173.90 to 183.50	12.437 to 22.615	24
Xiong et al. (2015)[11]	Static analytic method with sampling technique	T-P-x_V	CO_2-CH_4-3 mol.% N_2 CO_2-CH_4-5 mol.% N_2	153.15 to 193.15	2.670 to 22.00	77
			SLVE			
Riva and Stringari (2018)[14]	Static analytic approach	T-P-x_L-x_V	2 mol.% CO_2-58 mol.% CH_4-40 mol.% N_2 2 mol.% CO_2-79 mol.% CH_4-19 mol.% N_2	124.5 to 145.9	5.2 to 20.4	6

[a] as reported by Agrawal and Laverman.[8]

2.3 The CO_2-CH_4-N_2-O_2 system

Riva and Stringari[14] reported some data concerning SLVE of the quaternary mixture comprising CO_2, CH_4, N_2 and O_2 in order to better understand the influence of nitrogen and air content on phase equilibria. Table 4 summarizes the available data that, to our knowledge, are the only ones currently available for this system. More details on experimental data are reported in Tables S21-S22 in the *Supporting Information*.

Table 4. SLVE experimental data available in the literature for the CO_2-CH_4-N_2-O_2 mixture.

Literature source	Data type	Mixture composition	*T* [K]	*P* [bar]	No. points
Riva and Stringari (2018)[14]	T-P-x_L-x_V	2 mol.% CO_2-58 mol.% CH_4-31 mol.% N_2-9 mol.% O_2 2 mol.% CO_2-79 mol.% CH_4-15 mol.% N_2-4 mol.% O_2	125.1 to 146.5	5.8 to 21.1	6

3. Algorithm for the simultaneous computation of phase stability and multiphase equilibria for solid, liquid and vapor phases

In this section, an algorithm for the simultaneous computation of phase stability and multiphase equilibria of CO_2 mixtures with hydrocarbons and non-hydrocarbon components is presented. The proposed algorithm allows to overcome one of the common problems encountered in the calculation of phase equilibria (e.g., when based on the isofugacity condition)[21], i.e. that the number of phases which are present at equilibrium are not known *a-priori*. The adopted stability criterion was first presented in the literature by Gupta[22] as an alternative to other approaches (e.g., those proposed by Gautam and Seider,[23] Michelsen,[24-26] Wu and Bishnoi,[27] Castier et al.[28]). Gupta and co-authors applied such method to systems for which vapor-liquid-liquid equilibrium (VLLE) conditions can be established, such as the ethanol-ethyl acetate-water system[29] and the CO_2-CH_4-H_2S system.[30] This stability criterion was later applied by Ballard and Sloan[31] and by Segtovich et al.[32] to systems involving several phases of interest (including gas hydrates) in order to perform multiphase flashes. More recently, Tang and co-workers[33] have extended the algorithm developed by Gupta[22] to compute SVE, SLE and SLVE of the CO_2-CH_4 mixture. In their study, the fugacity coefficients of fluid phases (i.e., vapor and liquid) were calculated using GERG-2004 multi-parameter Equation of State (EoS), while the EoS that described the thermodynamic behavior of solid CO_2 was based on the Gibbs free energy method suggested by Jäger and Span.[34]

In this work, the approach proposed by Gupta[22] has been implemented in a Fortran code to couple phase stability and isothermal-isobaric flash calculations that involve the vapor, liquid and/or solid phases, with the latter one assumed to consist of pure CO_2. To our knowledge, this approach has never been applied to phase equilibria involving solid CO_2 for multicomponent systems and the difference with respect to previous literature works[33], focused on the CO_2-CH_4 binary system only, lies in the different thermodynamic models used for the properties of fluid phases and of solid CO_2. Indeed, in this work, the Peng Robinson EoS has been used for computing the fugacities of the fluid phases, whereas the fugacity of pure CO_2 in the solid phase has been expressed by relating it to the fugacity of pure CO_2 in the vapor phase, without any derivation from a hypothetical subcooled liquid fugacity. The implementation for multicomponent systems, the novelty of this work consists of, finds practical application in the study and correct design of many CO_2 removal processes operated at low-temperature/cryogenic conditions. For example, the proposed algorithm can be used to check if a mixture of interest will form solid CO_2 at certain temperature and pressure conditions, such as those at some trays of low-temperature distillation columns that have been recently studied for the sweetening of high CO_2-content natural gases[35] or for the upgrading of biogas.[36] Indeed, commercial simulation software often do not take into account the formation of CO_2(s). This is one of the possible applications of the proposed algorithm, which helps determining the operating conditions that ensure a correct operation of processes.

The theoretical background for the algorithm implemented in this work is outlined in the *Supporting Information*, for the sake of clarity. In the following, the implementation of the algorithm is discussed, which requires the following input data, as illustrated in Figure 1: temperature T, pressure P, and the global composition (z_i refers to the mole fraction of the i-th component in the feed stream).

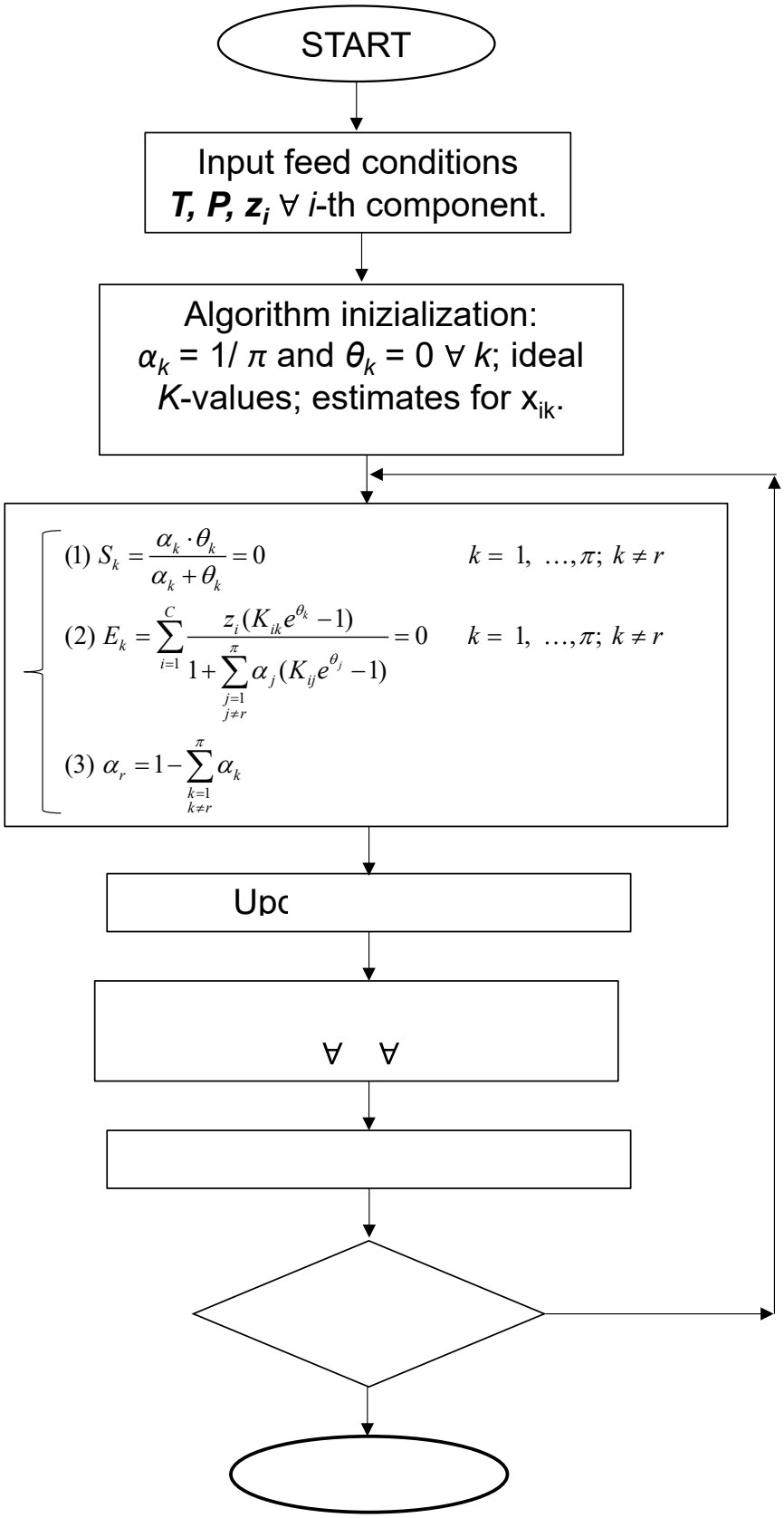

Figure 1. Block diagram of the proposed algorithm that simultaneously performs isothermal-isobaric flash calculations and a phase stability analysis.

The algorithm is started assuming all phases are present with an equal amount of each, and, therefore, their stability variables (θ_k) are all zero.[37] The inizialization of the Gibbs energy minimization algorithm also requires a set of *K*-values that are composition-independent (also commonly referred to as ideal *K*-values). The initial estimate for the mole fraction of each component (i = 1, …, C) in each phase (k = 1, …, π) has been computed according to eq S14 in the *Supporting Information*, where the molar phase fraction $\alpha_k = 1/\pi$ and the stability variable $\theta_k = 0$ for all k phases (k = 1, …, π) the implemented algorithm takes into account.

Then, the first part of the problem to be solved, which can be referred to as "inner loop", consists in minimizing the Gibbs free energy of the system at a given set of *K*-values and composition. The following system of (2π-1) equations is solved in the (2π-1) unknowns, α_k (k = 1, …, π) and θ_k (k = 1, …, π and $k \neq$ r).

$$\begin{cases} S_k = \dfrac{\alpha_k \cdot \theta_k}{\alpha_k + \theta_k} = 0 & for\ k = 1, \ldots, \pi \ \ and \ \ k \neq r \\ E_k = \displaystyle\sum_{i=1}^{C} \frac{z_i (K_{ik} e^{\theta_k} - 1)}{1 + \displaystyle\sum_{\substack{j=1 \\ j \neq r}}^{\pi} \alpha_j (K_{ij} e^{\theta_j} - 1)} = 0 & for\ k = 1, \ldots, \pi \ \ and \ \ k \neq r \\ \alpha_r = 1 - \displaystyle\sum_{\substack{k=1 \\ k \neq r}}^{\pi} \alpha_k \end{cases} \quad (1)$$

The Newton procedure is used to solve the above system, which requires expressing the derivatives of the equations above with respect to each unknown variable. To avoid incurring in a singular Jacobian during the iterations, the technique presented by Gupta et al.[30] has been implemented. It consists in selecting a small positive number, ε, set equal to 1e-10, so that whenever α_k becomes less or equal to ε while θ_k is zero, both α_k and θ_k are set equal to ε. The same occurs whenever θ_k becomes less or equal to ε while α_k is zero. For the special case in which both α_k and θ_k are less than ε, the solution of the system remains at the point $\alpha_k = \theta_k = \varepsilon$.

After the inner loop is solved and the values for α_k and θ_k are updated, it is, then, possible to calculate in the outer loop the mole fraction of each component (i = 1, …, C) in each phase (k = 1, …, π), using eq S14 reported in the *Supporting Information*. From this point on, the *K*-values are calculated removing the assumption according to which they were assumed composition-independent.

Recalling the definition of the *K*-values as the ratios of fugacity coefficients of component i between phase k and the reference phase r, it is necessary to define a *K*-value that corresponds to some reference phase. Their expressions are reported in Table 5, depending on which phase is taken as the reference one. As previously reported, the fugacity coefficients in the vapor and liquid phases have

been calculated with the Peng Robinson EoS.[38] On the contrary, the fugacity of pure solid CO_2 has been expressed using a model different from the one suggested by Jäger and Span[34] and by relating it to the one in the vapor phase, which requires computing its solid vapor pressure ($P_{subl,i}$ for $i = CO_2$ in Table 5) at the system temperature and the fugacity coefficient of CO_2 in the vapor phase at the system temperature and pressure, if the Poynting correction term is neglected. The dependence of the solid vapor pressure upon temperature can be expressed according to the 6-parameter correlation proposed by Jensen et al.,[39] which has been used in this work.

Calculations are performed until convergence is reached in the outer loop on the normalized composition of all phases. If convergence is not reached using a reference phase (the vapor phase is tried first), the calculation is repeated taking the liquid and, if needed, the solid phase as the reference one.

Table 5. Expressions for composition-dependent K_{ik} assuming different phases as the reference (r) phase.

K_{ik}	$r = V$	$r = L$	$r = S$
K_{iV}	$= \frac{x_{iV}}{x_{iV}} = 1$	$= \frac{x_{iV}}{x_{iL}} = \frac{\hat{\phi}_i^L(T,P,\mathbf{x}_L)}{\hat{\phi}_i^V(T,P,\mathbf{x}_V)}$	$\begin{cases} = \frac{x_{iV}}{x_{iS}} \to \infty & \text{for i} \neq \text{CO}_2 \\ = \frac{x_{iV}}{x_{iS}} = \frac{P_{subl,i}(T)\cdot\phi_i^V(T,P_{subl,i}(T))}{P\cdot\hat{\phi}_i^V(T,P,\mathbf{x}_V)} & \text{for i} = \text{CO}_2 \end{cases}$
K_{iL}	$= \frac{x_{iL}}{x_{iV}} = \frac{\hat{\phi}_i^V(T,P,\mathbf{x}_V)}{\hat{\phi}_i^L(T,P,\mathbf{x}_L)}$	$= \frac{x_{iL}}{x_{iL}} = 1$	$\begin{cases} = \frac{x_{iL}}{x_{iS}} \to \infty & \text{for i} \neq \text{CO}_2 \\ = \frac{x_{iL}}{x_{iS}} = \frac{P_{subl,i}(T)\cdot\phi_i^V(T,P_{subl,i}(T))}{P\cdot\hat{\phi}_i^L(T,P,\mathbf{x}_L)} & \text{for i} = \text{CO}_2 \end{cases}$
K_{iS}	$\begin{cases} 0 & \text{for i} \neq \text{CO}_2 \\ = \frac{x_{iS}}{x_{iV}} = \frac{P\cdot\hat{\phi}_i^V(T,P,\mathbf{x}_V)}{P_{subl,i}(T)\cdot\phi_i^V(T,P_{subl,i}(T))} & \text{for i} = \text{CO}_2 \end{cases}$	$\begin{cases} 0 & \text{for i} \neq \text{CO}_2 \\ = \frac{x_{iS}}{x_{iL}} = \frac{P\cdot\hat{\phi}_i^L(T,P,\mathbf{x}_L)}{P_{subl,i}(T)\cdot\phi_i^V(T,P_{subl,i}(T))} & \text{for i} = \text{CO}_2 \end{cases}$	$= \frac{x_{iS}}{x_{iS}} = 1$

In this work, two types of phase equilibrium problems are investigated concerning SVE and SLVE conditions.

When SVE conditions are given in the literature in terms of CO_2 frost points as *T*, *P* pairs, the calculation has been carried out at the same global composition (typically available) and pressure as the experimental ones, whereas the temperature has been varied so that the highest value for which the CO_2 solidification ratio (corresponding to the ratio α_S/z_{CO2}) is greater than or equal to 0.0001 is considered as the temperature of frost point. Such calculated temperature is compared with the experimental one reported in the literature.

Considering the datasets reporting SVE measurements as P-$x_{CO2,V}$ at a given temperature, these do not always include the global composition of the mixture charged into the equilibrium cell. This is the case, for example, for some data available in the literature for the CO_2-CH_4 binary mixture.[6, 11] Therefore, to provide the required input data to the Fortran code, it has been necessary to assume a global composition for the system. To do that, the behavior of the CO_2-CH_4 binary system has been taken into account, which is shown, for the sake of clarity, in the *P*-composition diagrams in Figure 2 for the two temperatures of 178.15 K and 203.15 K (respectively, lower and higher than the critical temperature of methane, i.e. 190.6 K[40]). These two diagrams have been constructed by running the Fortran code several times with different input data. Since the temperature is fixed (at, respectively, 178.15 K and 203.15 K in Figure 2a and in Figure 2b), the overall composition has been assigned (starting, for example, from an equimolar mixture of the two components) and the isothermal-isobaric flash has been solved for different input values of the pressure (read from an array), obtaining the phases present at equilibrium and their composition, which is plotted in Figure 2. The same procedure has been followed by changing the input global composition so that all types of equilibria (e.g., also the small VLE region) could be shown. The two diagrams in Figure 2 are qualitatively representative of the same diagrams at temperatures, respectively, lower and higher than the critical temperature of methane. Therefore, based on this behavior, when considering the datasets reporting SVE measurements as P-$x_{CO2,V}$ at a given temperature, the global composition has been assigned setting the CO_2 mole fraction at a value higher than the mole fraction in the vapor phase at equilibrium as determined experimentally.

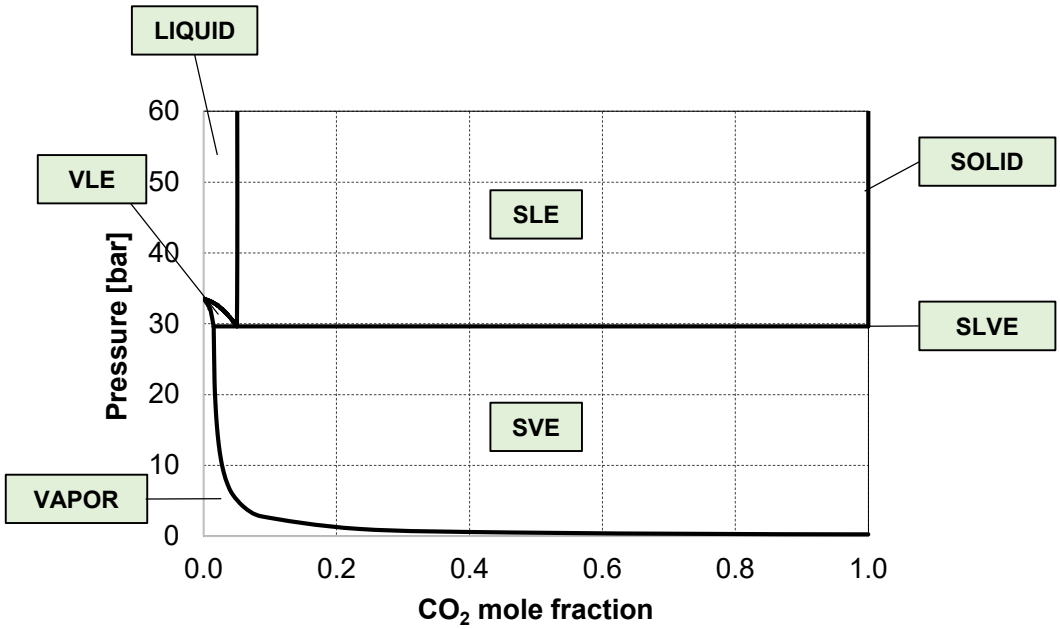

a)

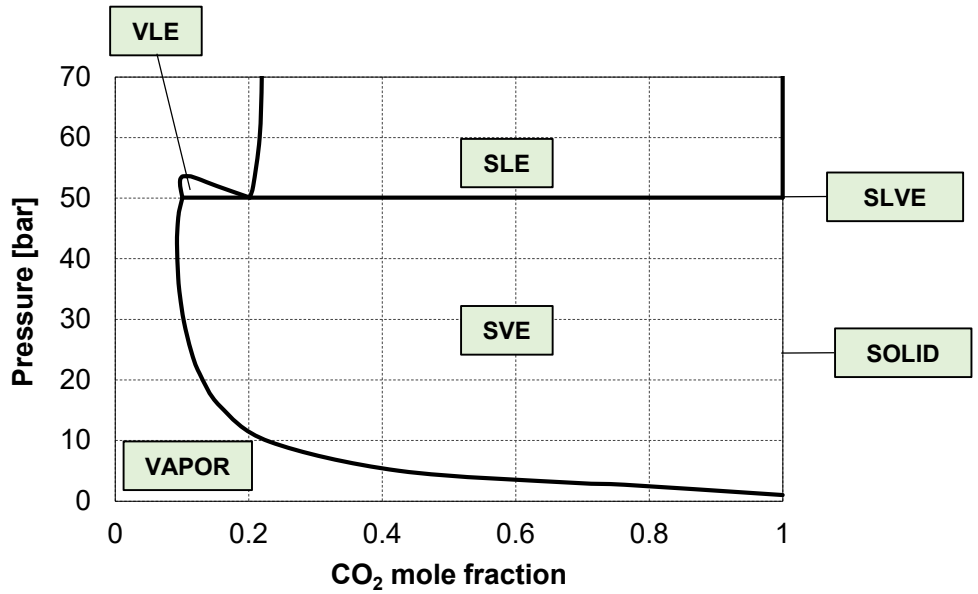

b)

Figure 2. Pressure-composition diagram constructed using the proposed algorithm for the CO_2-CH_4 binary mixture at: a) 178.15 K; b) 203.15 K.

For the ternary mixture, the SVE data collected by Xiong and co-workers[11] are given in terms of temperature, pressure, composition of the vapor phase at equilibrium and a given mole fraction of N_2 in the ternary mixture (i.e., 3 mol.% or 5 mol.%). In this case, the global composition has been assigned considering the given mole fraction of N_2 and a mole fraction of CO_2 greater than the one in the vapor phase at equilibrium.

To use the proposed algorithm for SLVE calculations for the CO_2-CH_4 binary mixture and for ternary and quaternary mixtures also containing N_2 and O_2, this procedure has been followed. As for the

binary mixture, a global composition has been assumed and, at a given temperature set equal to the available experimental value, the SLVE pressure has been determined. In fact, for the binary mixture, at a fixed temperature, SLVE conditions are established at a unique pressure. This is not the case if the pressure were fixed instead, due to the maximum shape of the SLVE locus for the CO_2-CH_4 mixture (as shown in the following in Figure 7), which implies that for certain pressures there exist two temperatures at which dry ice can coexist with the vapor and liquid phases.

In the case of mixtures also containing nitrogen and/or oxygen, when the global composition, the temperature and the pressure are reported in the literature,[14] all the input data required by the proposed algorithm are available. Therefore, it is possible to use it to calculate the composition of the phases present at equilibrium and make a comparison with that available in the literature.

The results are reported in the following together with those that can be obtained using the RGibbs tool[41] available in Aspen Plus® V9.0.[42] To our knowledge, it is the only unit operation that is able to deal with this type of phase equilibria: it uses Gibbs energy minimization techniques to compute equilibrium instead of methods based on the equality of the fugacity of each component in each phase. The system is considered at equilibrium when the distribution of the components of a system is obtained such that the Gibbs energy is minimal (subject to atom balance constraints). According to the literature from Aspen Technology, the method based on Gibbs energy minimization can be used for any number of phases and components and always yields stable solutions. To be consistent with the models our algorithm makes use of, we have selected the Peng Robinson EoS, which applies to fluid phases. To calculate enthalpies, entropies, and Gibbs free energies for conventional components in the vapor and/or liquid phase, the simulator uses standard heat of formation and standard Gibbs free energy of formation. On the contrary, the standard solid heat of formation and standard solid Gibbs free energy of formation for the component of "solid" type (i.e., solid CO_2) present in our simulation need to be specified. Then, other properties (for which the default options have been kept) are used by the simulator to calculate each property at a given temperature and pressure.

4. Results and discussion

In this section, the results obtained with the proposed algorithm are discussed taking into account the average absolute deviation (AAD%) calculated according to the generic equation:

$$AAD\% = \frac{100}{n}\sum_{i=1}^{n}\frac{\left|v_{calc,i} - v_{\exp.i}\right|}{v_{\exp.i}} \qquad (2)$$

where v_{calc} refers to the calculated value of the generic variable (e.g., the temperature in case of CO_2 frost point calculations), v_{exp} refers to the experimental value of the same generic variable, and n stands for the number of experimental available data.

In the following, the results for the CO_2-CH_4 binary mixture are illustrated first (section 4.1). Then, in sections 4.2-4.3, the results obtained for mixtures also containing nitrogen and oxygen are shown. The experimental data are reported with the corresponding error bar, when this information was available in the literature.

4.1 The CO_2-CH_4 system

Results for the calculation of frost point temperatures are illustrated in Figure 3. The AAD% for each literature source is reported in Table 6.

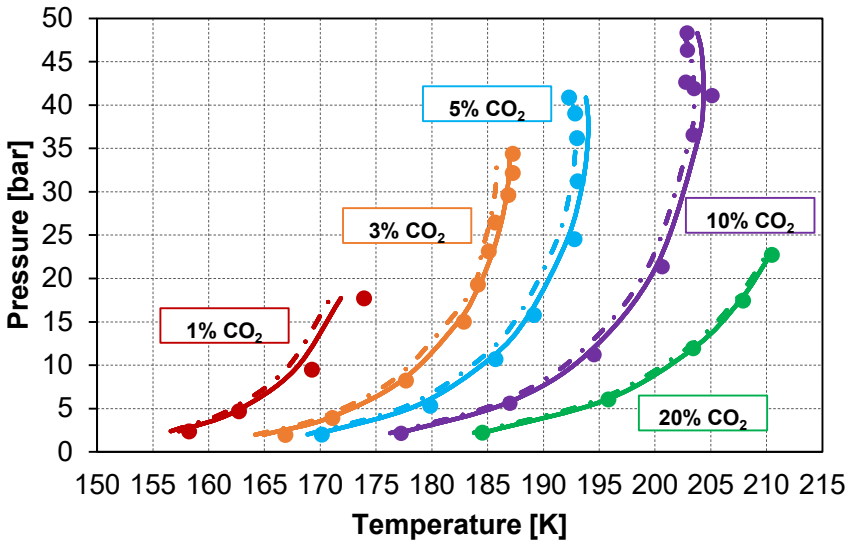

a)

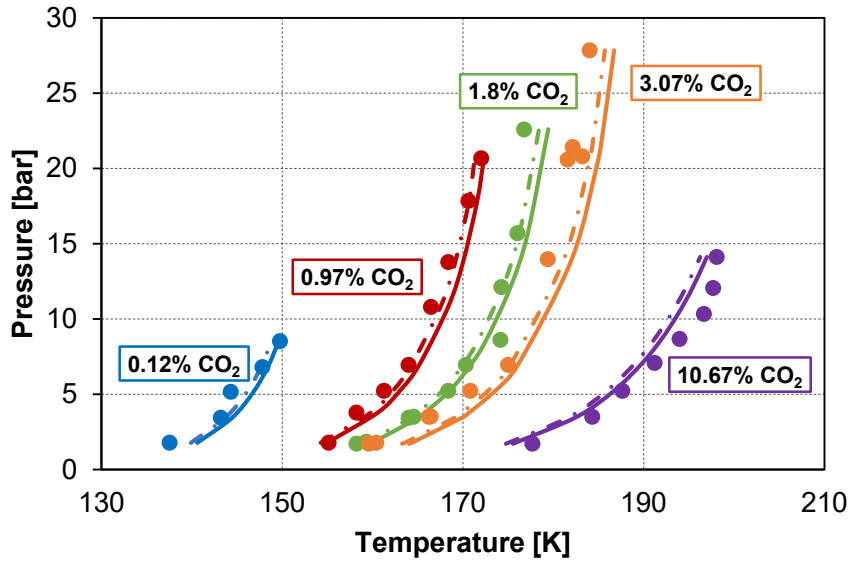

b)

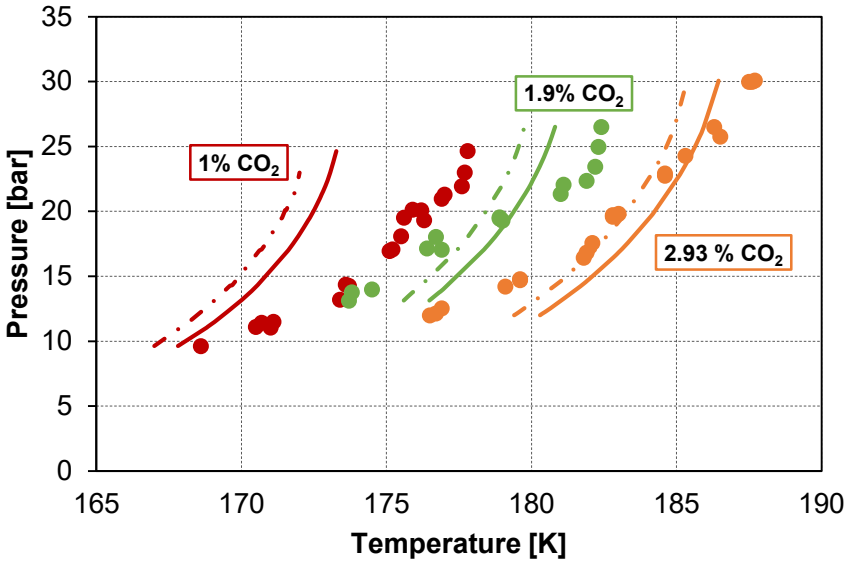

c)

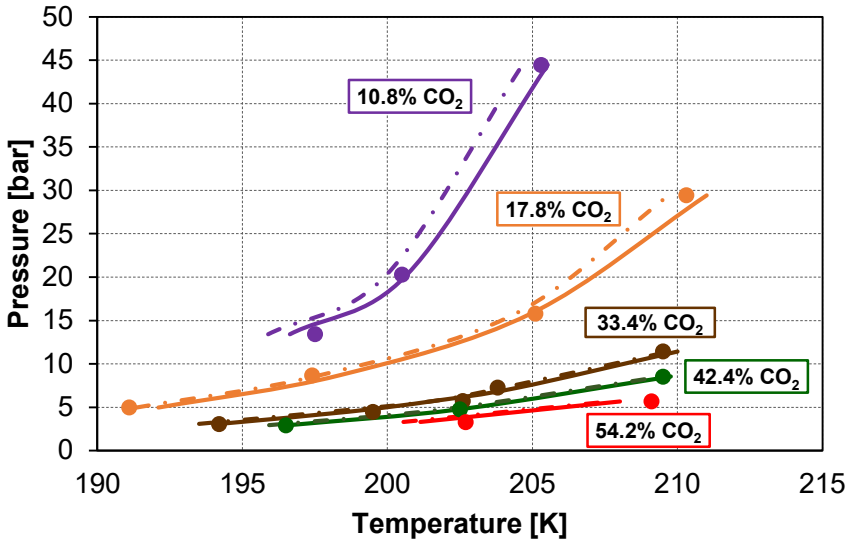

d)

Figure 3. Comparison between the results obtained with the proposed algorithm (solid line), by simulation with RGibbs in Aspen Plus® V9.0[42] (dashed and dotted line), and the experimental data of frost points for the CO_2-CH_4 mixture for different datasets: a) Pikaar;[6] b) Agrawal and Laverman;[8] c) Le and Trebble;[7] d) Zhang et al.[9]

Table 6. AAD% (eq 2) in the calculation of frost points for the CO_2-CH_4 mixture.

Literature Source	This work	RGibbs
Pikaar (1959)[6]	0.360	0.574
Agrawal and Laverman (1995)[8]	1.079	0.873
Le and Trebble (2007)[7]	1.239	1.364
Zhang et al. (2011)[9]	0.297	0.375

Figure 4 shows the results for SVE calculations on *P*-composition diagrams. It is possible to observe that there exists a good agreement between the two different approaches and the experimental data, with an overall AAD% equal to 5.86 % for the proposed algorithm and 5.04 % for the RGibbs tool when considering the dataset by Pikaar[6] and, respectively, 7.61 % and 8.34 % when considering the dataset by Xiong et al.[11] In particular, higher deviations are observed at low concentrations, as illustrated in Figure 5, which presents percentage differences between CO_2 *K*-values from calculations and data plotted against the mole percentage of CO_2 in the vapor phase. Indeed, when considering the proposed approach the calculated *K*-values agree with the experimental data to within ± 14% at high concentrations and temperatures (203.15 K to 173.15 K, Figures 5a-d), whereas they agree to within ± 32% at low concentrations and temperatures (168.15 K and 153.15 K in Figures 5e-f). This may be also due to greater uncertainties of the experimental data at these conditions. It is also interesting to notice that larger deviations are observed, considering the same composition range and temperature, for the data by Xiong et al.[11] (Figure 5b and Figure 5f). Indeed, at the lowest CO_2 concentrations and temperature (Figure 5f), the *K*-values calculated with the proposed approach are underestimated by maximum 7.5 % with the experimental data by Pikaar[6] only (i.e., by neglecting the data by Xiong et al.[11]). These difference may be explained considering that the experimental procedure used in the two works is different, as well as the analysis technique. Pikaar[6] used a saturation cell apparatus whose walls were coated at the beginning with solid CO_2 and in which some methane was fed, after cooling to the cryostat temperature; then, the saturated methane left the cell, was warmed to room temperature outside the bath and expanded to atmospheric pressure; the samples were analyzed by infra-red absorption. Xiong et al.[11] performed their measurements by first filling the equilibrium cell with the test gas mixture as to guarantee the CO_2 content in it to be slightly higher than the predicted content at frost point. Then, they filled the constant temperature bath with helium and the container with liquid nitrogen, set the temperature and waited for equilibrium to be reached, sampled the gas mixture and analyzed its composition by a gas chromatograph.

Moreover, since the agreement between calculated results and experimental data in Figure 4 is less satisfactory at higher pressures, we investigated the effect due to the Poynting correction factor that has not been taken into account in the expression of K_{iS} in Table 5. If that expression is modified as in eqs. 3 to 4, where the solid molar volume (v_S) has been taken from the literature,[41] then the AAD% for the proposed algorithm decreases to 3.74 % and 7.47 %, respectively, for the two datasets presented by Pikaar[6] and Xiong et al.[11], allowing to obtain better performances, in particular for the dataset presented by Pikaar.[6]

$$K_{iS}(r=V) \begin{cases} 0 & \text{for i} \neq CO_2 \\ = \dfrac{x_{iS}}{x_{iV}} = \dfrac{P \cdot \hat{\phi}_i^V(T,P,\mathbf{x}_V)}{P_{subl,i}(T) \cdot \phi_i^V(T,P_{subl,i}(T)) \exp\left[\dfrac{v_{iS}(P-P_{subl,i}(T))}{RT}\right]} & \text{for i} = CO_2 \end{cases} \quad (3)$$

$$K_{iS}(r=L) \begin{cases} 0 & \text{for i} \neq CO_2 \\ = \dfrac{x_{iS}}{x_{iL}} = \dfrac{P \cdot \hat{\phi}_i^L(T,P,\mathbf{x}_L)}{P_{subl,i}(T) \cdot \phi_i^V(T,P_{subl,i}(T)) \exp\left[\dfrac{v_{iS}(P-P_{subl,i}(T))}{RT}\right]} & \text{for i} = CO_2 \end{cases} \quad (4)$$

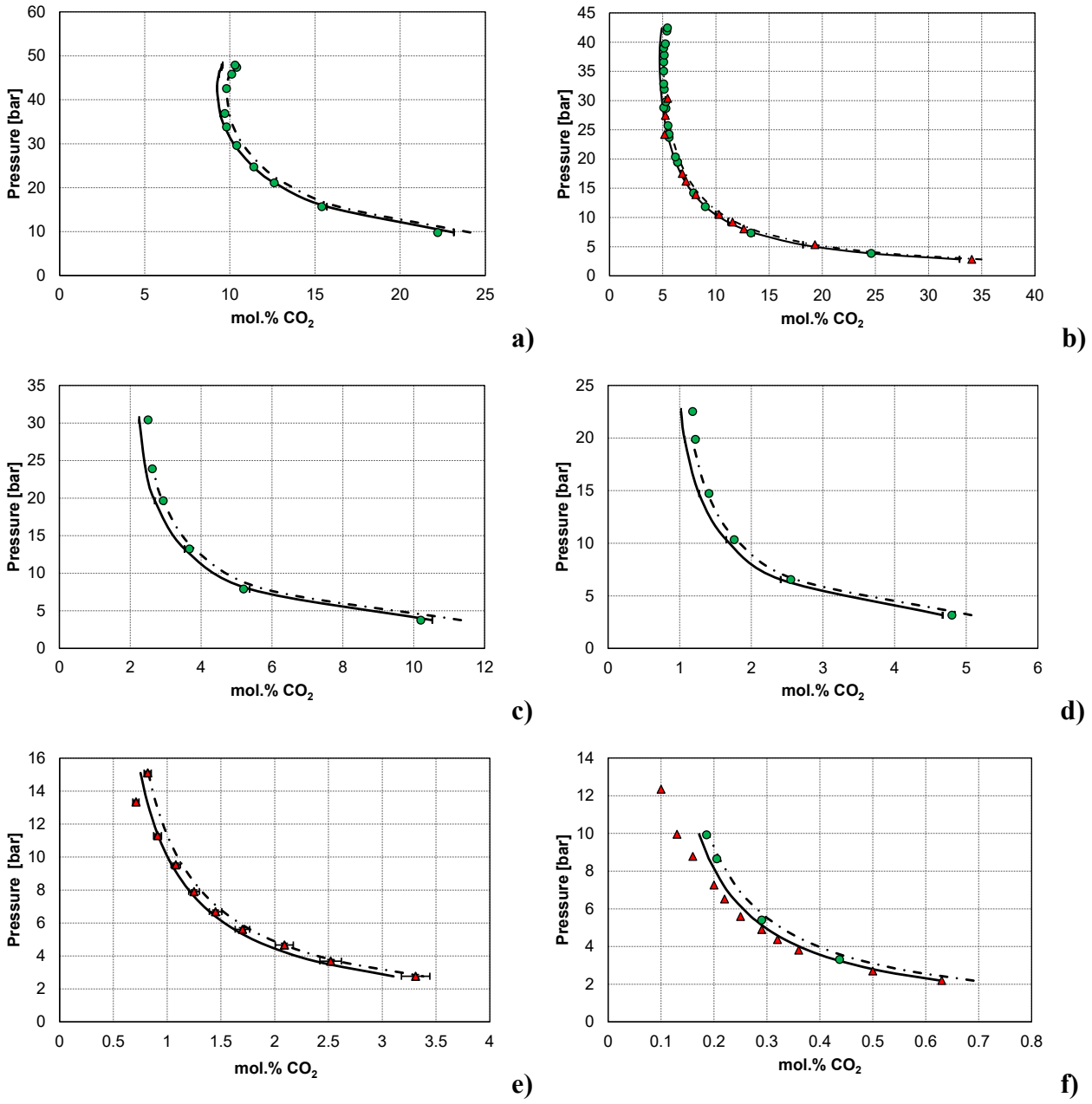

Figure 4. Comparison between the results obtained with the proposed algorithm (solid line) and by simulation with RGibbs in Aspen Plus® V9.0[42] (dashed and dotted line), and the experimental SVE data for the CO_2-CH_4 system (green dots: data by Pikaar;[6] red triangles: data by Xiong et al.[11]) at different temperatures: a) 203.15 K; b) 193.15 K; c) 183.15 K; d) 173.15 K; e) 168.15 K; f) 153.15 K.

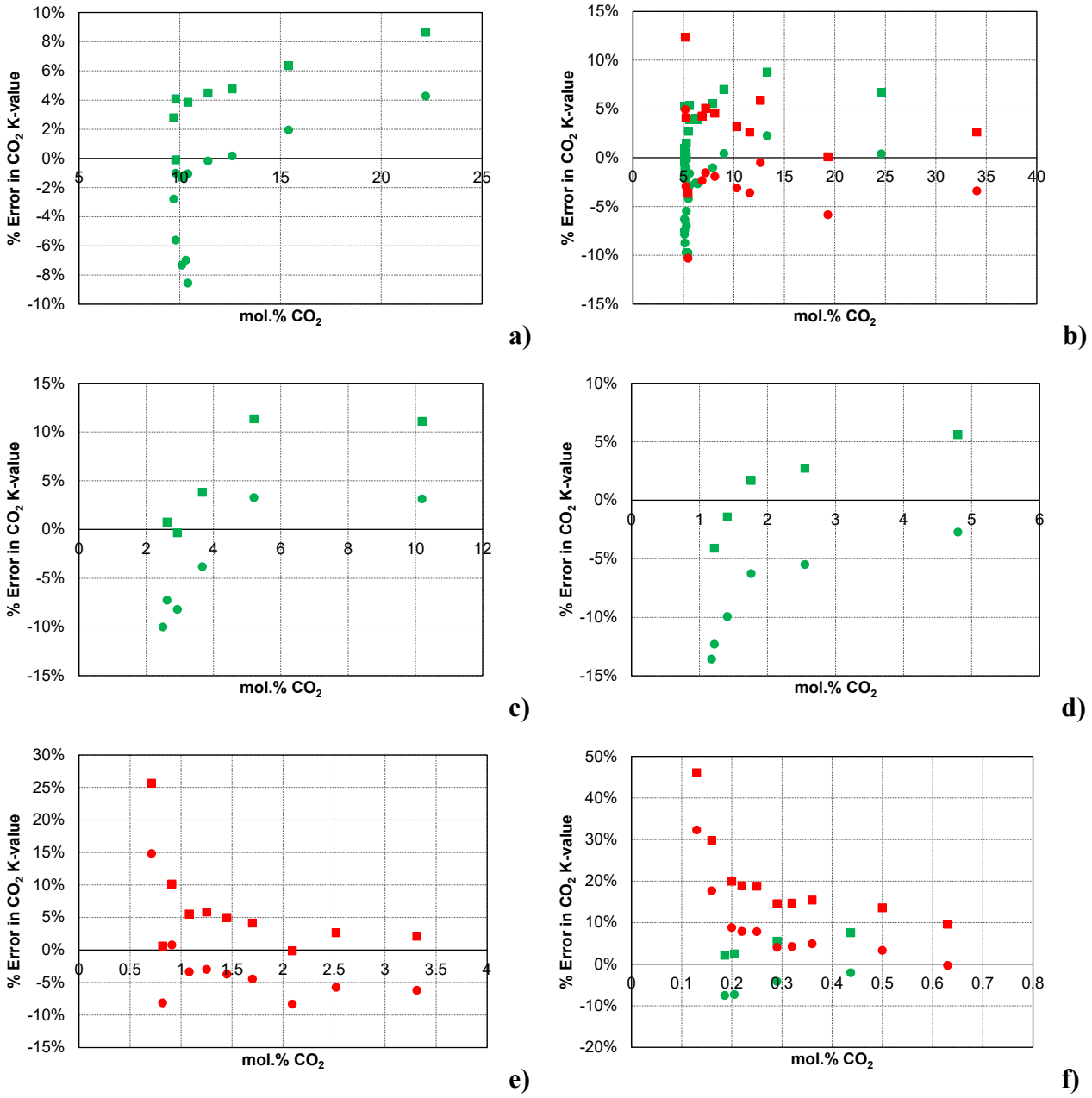

Figure 5. Percentage errors of *K*-value of CO_2 obtained with the proposed algorithm (●) and by simulation of RGibbs in Aspen Plus® V9.0[42] (■) in comparison to the SVE experimental data by Pikaar[6] (green) and by Xiong et al.[11] (red) at different temperatures: a) 203.15 K; b) 193.15 K; c) 183.15 K; d) 173.15 K; e) 168.15 K; f) 153.15 K.

Focusing the attention on Figure 3c, it is possible to observe that the results obtained with both approaches differ from the experimental data provided by Le and Trebble.[7] To achieve a better understanding of this, experimental frost point data from different literature sources at similar global composition have been compared, as shown in Figure 6.

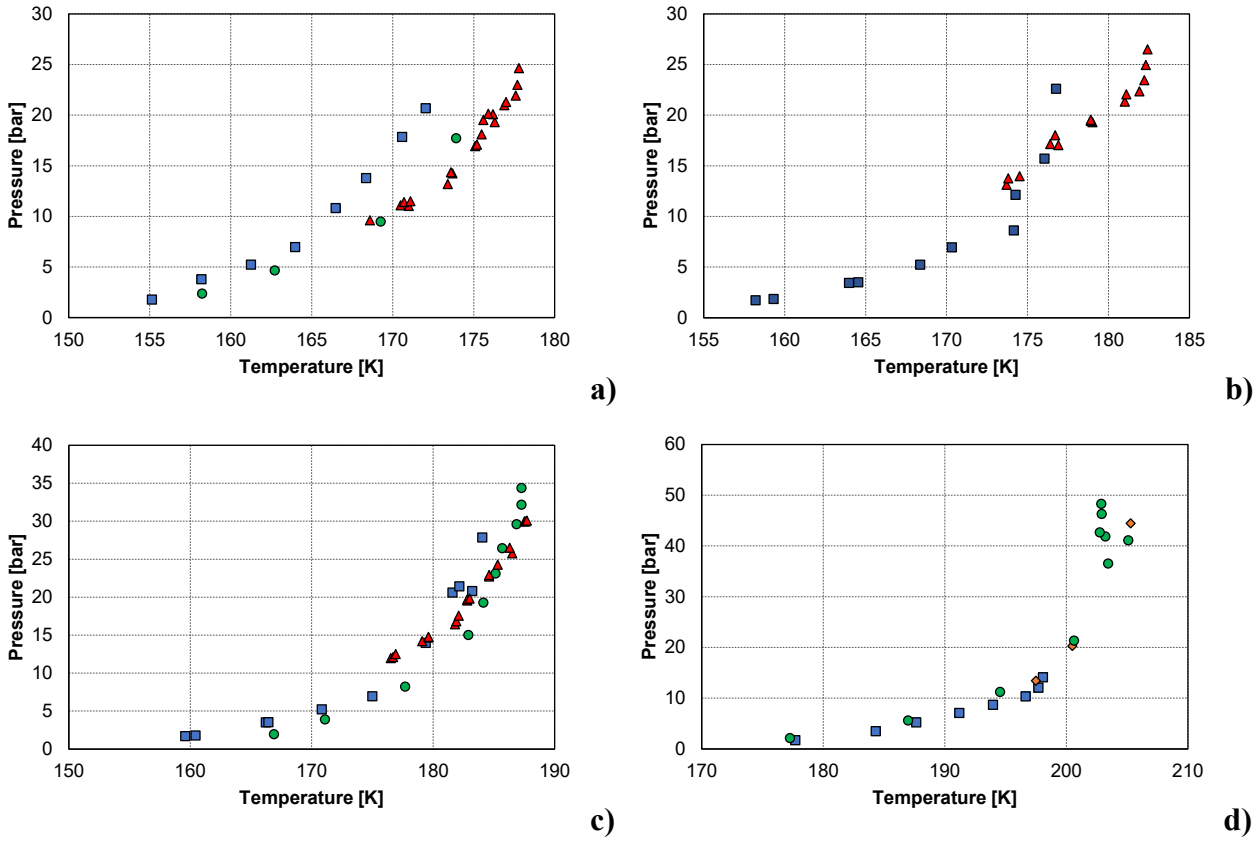

Figure 6. Comparison of the experimental frost point data for the CO_2-CH_4 system by Pikaar[6] (green dots), Agrawal and Laverman[8] (blue squares), Le and Trebble[7] (red triangles), and Zhang et al.[9] (orange diamonds) for four different global compositions: a) around 1 mol.% CO_2; b) around 2 mol.% CO_2; c) around 3 mol.% CO_2; d) around 10 mol.% CO_2.

As can be noticed from Figure 6, at higher pressures and lower amounts of carbon dioxide in the initial mixture, where the largest disagreement exists, the data collected by Le and Trebble[7] lie more closely to the data collected by Pikaar[6] and both are shifted to the right with respect to the data of Agrawal and Laverman.[8] However, the experimental data reported by Pikaar[6] cover a lower pressure range (from 2 to 18 bar) with respect to the ones presented by Le and Trebble[7] (from 9 to 25 bar), with only two points from Pikaar[6] in the same pressure range. Therefore, it is not possible to state if some of the datasets available in the literature are not reliable. On the contrary, at higher amounts of carbon dioxide (Figures 6c-d) the experimental data reported by the different authors are very close to each other.

As for the SLVE locus for the CO_2-CH_4 system, results are shown in Figure 7. The results obtained with the proposed algorithm (solid line) are in good agreement with the experimental data, except for those by Donnelly and Katz,[15] which however deviate from the other experimental data. Indeed, the locus of triple points by Donnelly and Katz[15] results to be lower in pressure or, conversely, higher in temperature than the results obtained with the proposed algorithm. As for the two calculation

approaches, some differences are observed at higher temperature values (i.e., above 195 K), where the SLVE locus obtained using the RGibbs tool lies below the locus obtained using the proposed algorithm. The AAD% for the proposed algorithm and the RGibbs tool are, respectively, 4.27 % and 8.94 % if all the available data are considered, whereas lower values are obtained (respectively, 2.20 % and 4.81 % for the two approaches) if the data from Donnelly and Katz[15] are not taken into account. Figure 8 shows the results for each experimental dataset. Since the Peng Robinson EoS[38] has been used as thermodynamic model for the fluid phases both in the proposed algorithm and in the set-up of the simulation in Aspen Plus® using the RGibbs tool, the differences observed in the results obtained with the two approaches can be explained considering that they are based on different models for calculating the fugacity and the properties of the solid phase (i.e., pure solid CO_2).

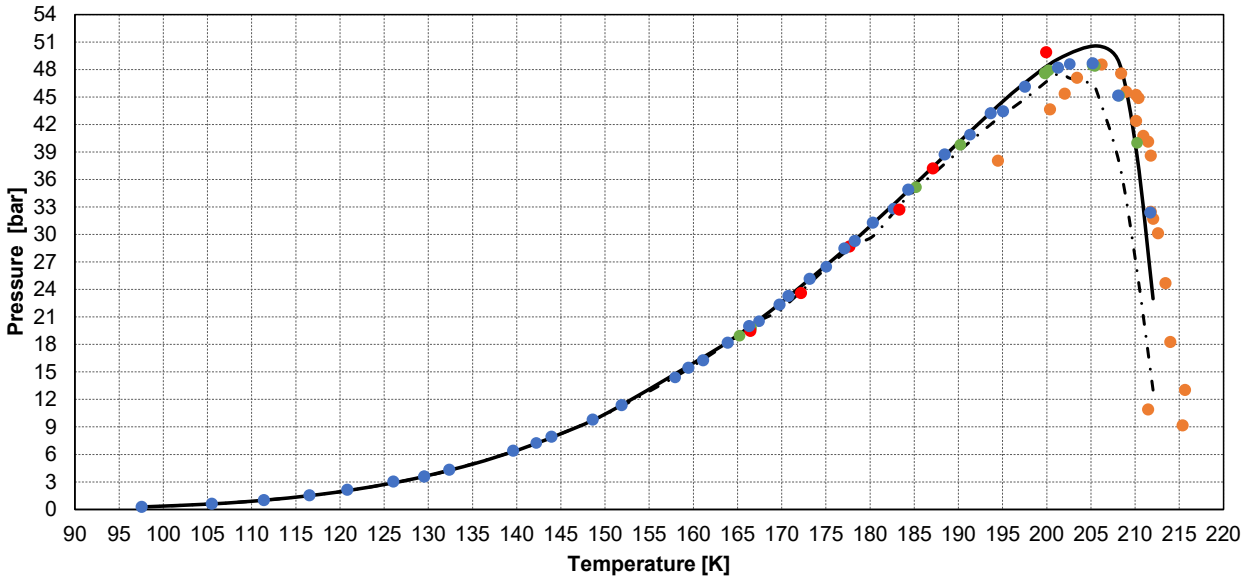

Figure 7. SLVE pressure as a function of temperature: comparison between the results obtained with the proposed algorithm (solid line), with the RGibbs tool of Aspen Plus® V9.0[42] (dashed and dotted line) and the experimental data available in the literature. The different colors refer to different works: orange, Donnelly and Katz;[15] red, Sterner;[16] light blue, Davis et al.;[17] green, Im and Kurata.[18]

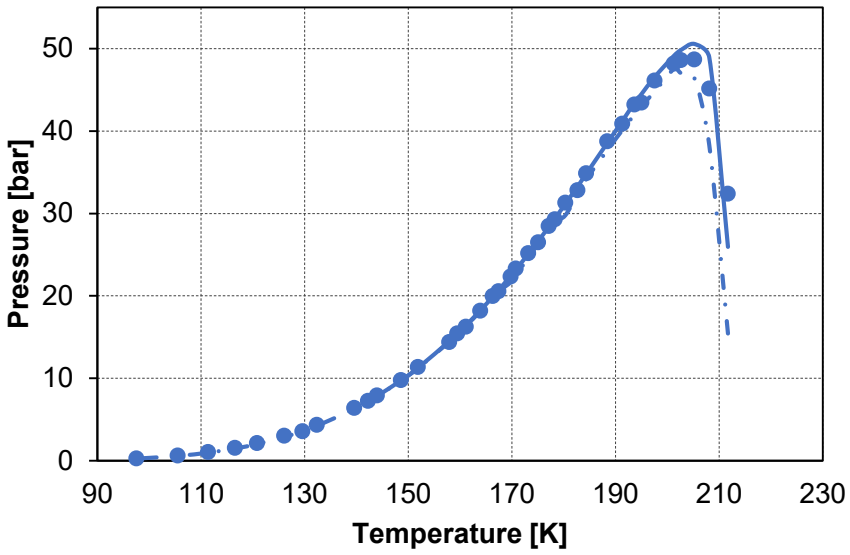
Pressure [bar]
0
10
20
30
40
50
90
110
130
150
170
190
210
230
Temperature [K]

a)

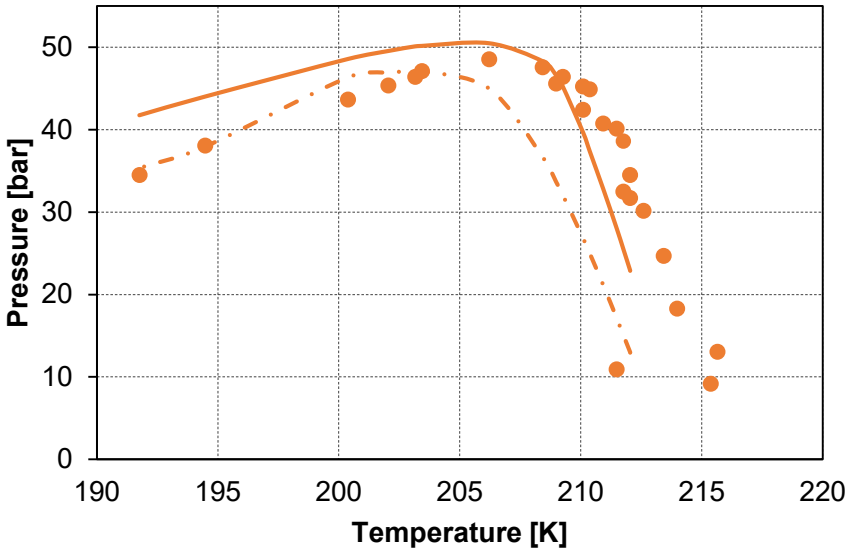
Pressure [bar]
0
10
20
30
40
50
190
195
200
205
210
215
220
Temperature [K]

b)

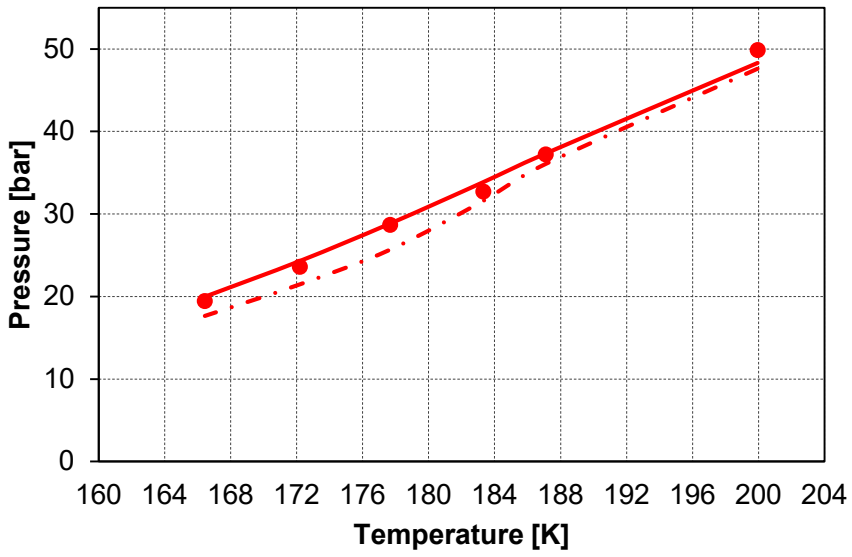

c)

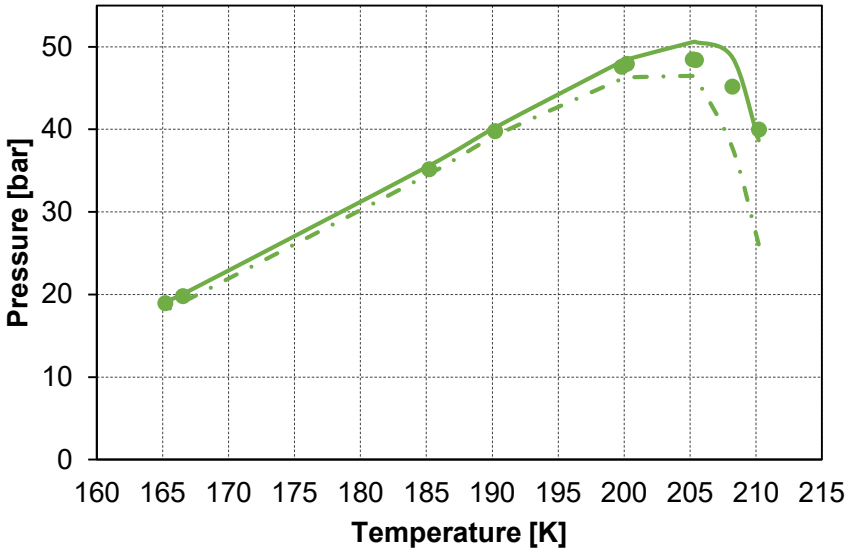

d)

Figure 8. SLVE pressure as a function of temperature: comparison between the results obtained with the proposed algorithm (solid line), with the RGibbs tool of Aspen Plus® V9.0[42] (dashed and dotted line) and the experimental data reported by: a) Davis et al.;[17] b) Donnelly and Katz;[15] c) Sterner;[16] d) Im and Kurata.[18]

Calculations have been also performed for the equilibrium composition of the vapor and liquid phases as a function of temperature and the results are illustrated in Figure 9. For the data for which only the temperature and mole fraction of CO_2 were available in the literature, the pressure has been set equal to the value obtained by using each calculation method. Calculation results are in good agreement with the experimental data, to a greater extent as for the composition of the vapor phase.

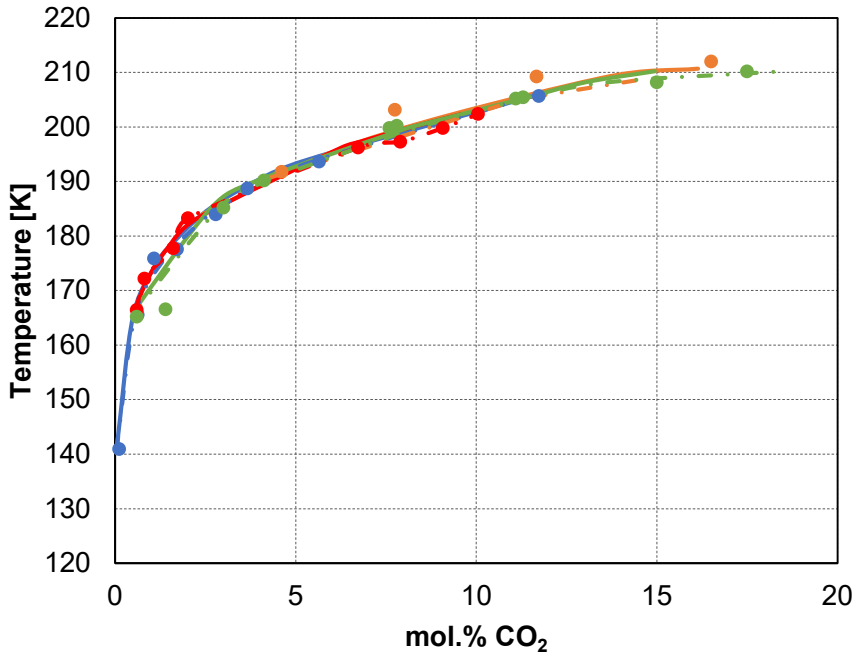

a)

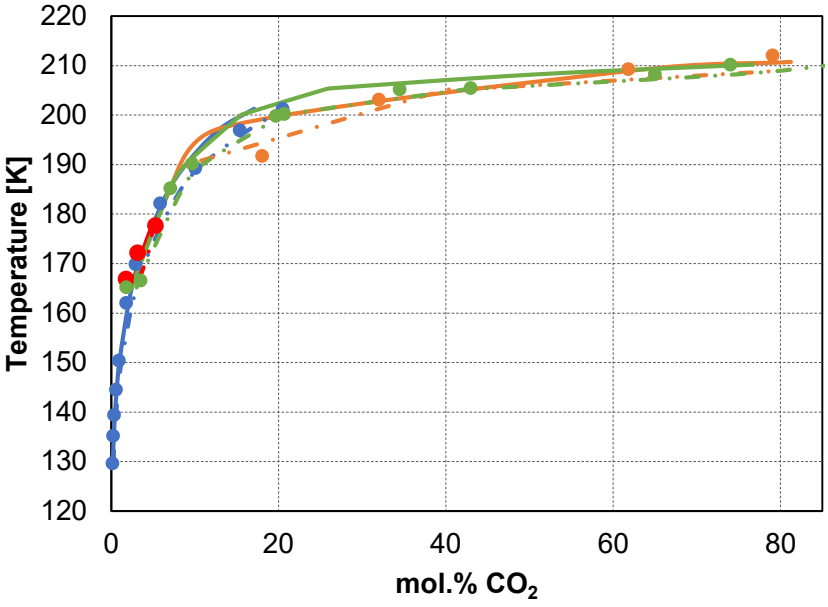

b)

Figure 9. Mole percentage of CO_2 as a function of temperature in: a) vapor phase at SLVE; b) liquid phase at SLVE. Comparison between the results obtained with the proposed algorithm (solid lines), by using the RGibbs tool of Aspen Plus® V9.0[42] (dashed and dotted line) and experimental data. The different colors refer to different literature sources: orange, Donnelly and Katz;[15] red, Sterner;[16] light blue, Davis et al.;[17] green, Im and Kurata.[18]

4.2 The CO_2-CH_4-N_2 system

Results for frost point calculations for the CO_2-CH_4-N_2 ternary mixture are illustrated in Figure 10 and in Figure 11 considering the datasets presented, respectively, by Agrawal and Laverman[8] and by Le and Trebble.[7] Focusing on Figure 10, it is possible to observe that both approaches and, in particular, the proposed one, are conservative in the prediction of the CO_2 frost point temperature. If Figure 11 is taken into account, it is possible to observe that the results obtained with both approaches deviate from the experimental data provided by Le and Trebble,[7] but the overall AAD% is still acceptable (0.91 % and 0.94 %, respectively, for the proposed algorithm and the RGibbs tool).

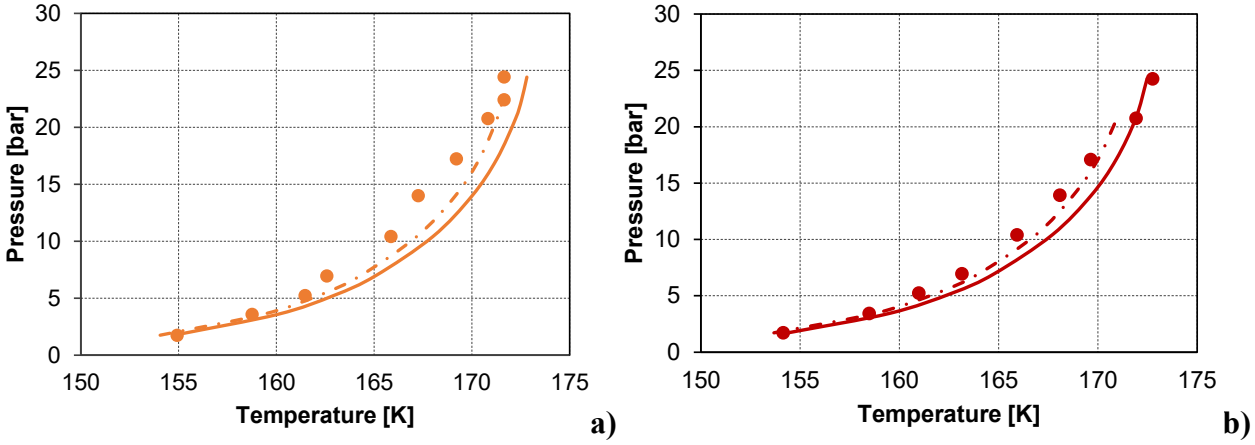

Figure 10. Comparison between the results obtained with the proposed algorithm (solid line), by simulation with RGibbs in Aspen Plus® V9.0[42] (dashed and dotted line) and the experimental frost point data for the CO_2-CH_4-N_2 system by Agrawal and Laverman[8] for two different CO_2-CH_4-N_2 mixtures: a) 0.96 mol.% CO_2, 98.36 mol.% CH_4, 0.68 mol.% N_2; b) 0.93 mol.% CO_2, 96.13 mol.% CH_4, 2.94 mol.% N_2.

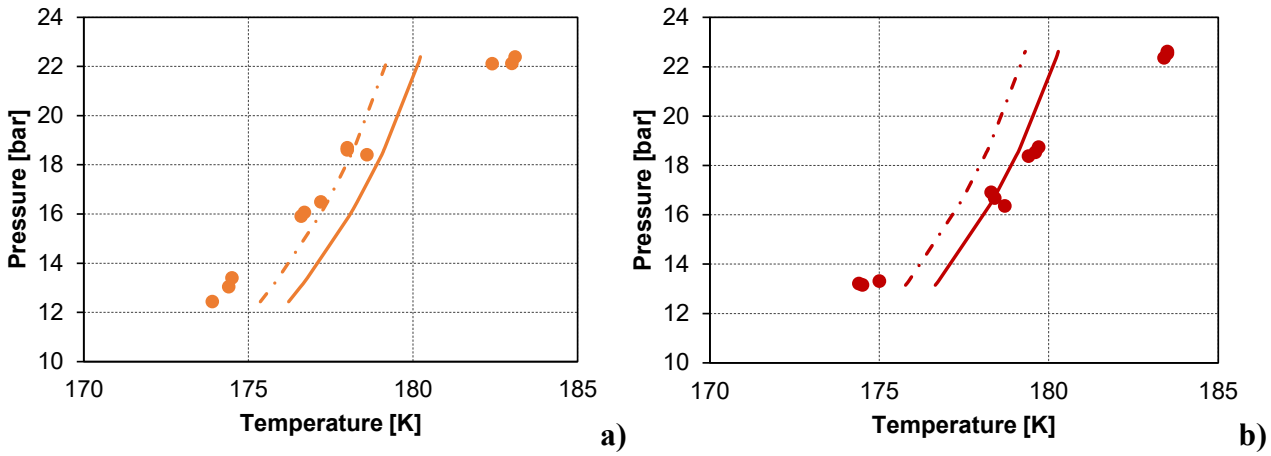

Figure 11. Comparison between the results obtained with the proposed algorithm (solid line), by simulation with RGibbs in Aspen Plus® V9.0[42] (dashed and dotted line) and the experimental frost point data for the CO_2-CH_4-N_2 system by Le and Trebble[7] for two different CO_2-CH_4-N_2 mixtures: a) 1.94 mol.% CO_2, 97.06 mol.% CH_4, 1 mol.% N_2; b) 1.94 mol.% CO_2, 96.11 mol.% CH_4, 1.95 mol.% N_2.

The results of the calculations performed for the SVE data reported by Xiong et al.[11] are shown in Figure 12 for the five given temperatures and the two mixtures containing, respectively, 3 mol.% (Figure 12a) and 5 mol.% N_2 (Figure 12b). The results from calculations agree with the experimental data and confirm the experimental evidence according to which with the increase of the nitrogen content, the maximum pressure for CO_2 desublimation increases as well.[11]

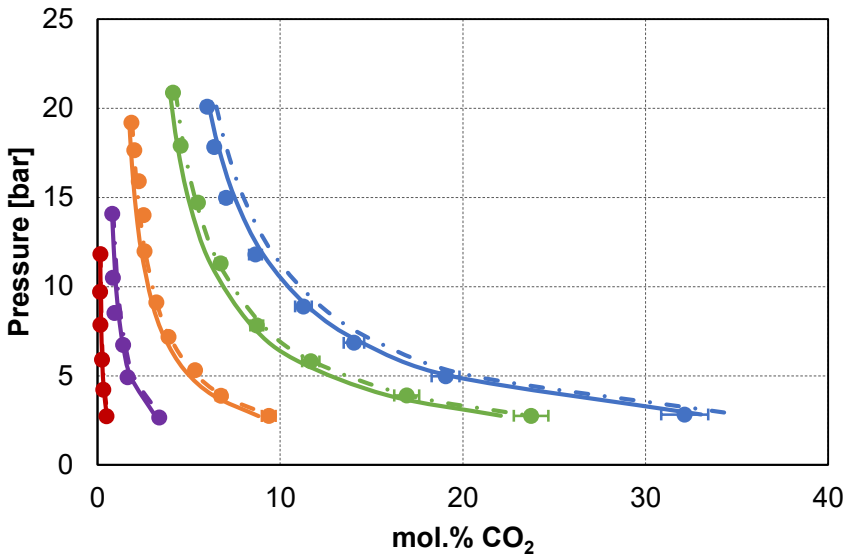

a)

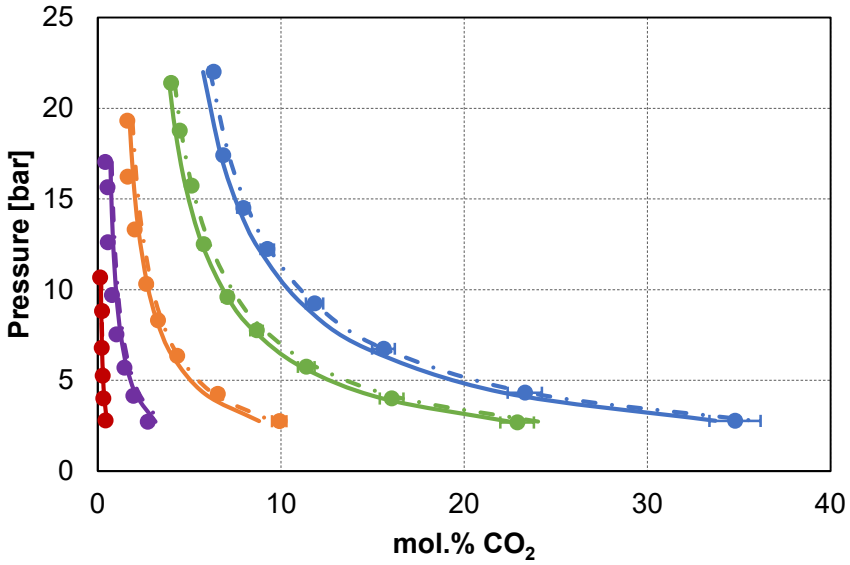

b)

Figure 12. Comparison between the results obtained with the proposed algorithm (solid line), by simulation of RGibbs in Aspen Plus® V9.0[42] (dashed and dotted line) and the SVE experimental data by Xiong et al.[11] for the: a) CO_2-CH_4-3 mol.% N_2 mixture; b) CO_2-CH_4-5 mol.% N_2 mixture. The different colors refer to five different temperatures: 193.15 K (light blue); 188.15 K (green); 178.15 K (orange); 168.15 K (purple); 153.15 K (red).

The SLVE for the CO_2-CH_4-N_2 system has been investigated by Riva and Stringari,[14] who presented experimental data for two mixtures as well as the results of their calculation approach. Such an approach is based on the isofugacity of the solid former component (i.e., CO_2) in the liquid, vapor and solid phases, which can be assumed as pure CO_2, and makes use of the GERG 2008 multi-parameter EoS for computing the fugacity in the fluid phases, while the fugacity of the solid phase has been calculated using the model reported by Jäger and Span.[34] Figures 13-14 compare the results obtained with the proposed algorithm with those obtained by Riva and Stringari,[14] and by the RGibbs tool for the two mixtures. It is possible to observe that the proposed algorithm (solid line) shows the best performances among the three ones, since the other two approaches tend to overestimate the CO_2 content in both fluid phases at SLVE conditions.

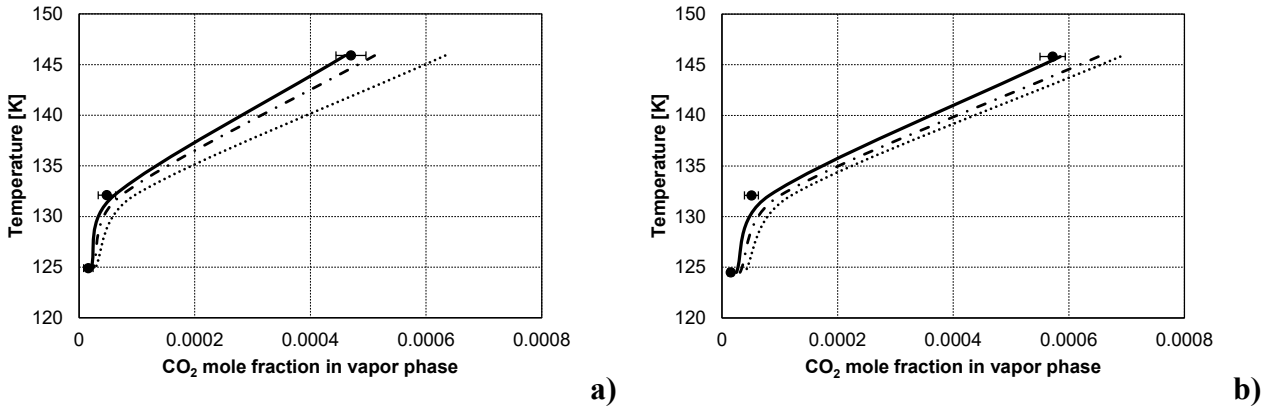

Figure 13. CO_2 mole fraction in the vapor phase at SLVE conditions for the CO_2-CH_4-N_2 system: comparison between the results obtained with the proposed algorithm (solid line), by simulation of RGibbs in Aspen Plus® V9.0[42] (dashed and dotted line), and by Riva and Stringari[14] (dotted line). Two mixtures are considered: a) Mixture 1: 2 mol.% CO_2, 58 mol.% CH_4, 40 mol.% N_2; b) Mixture 2: 2 mol.% CO_2, 79 mol.% CH_4, 19 mol.% N_2.

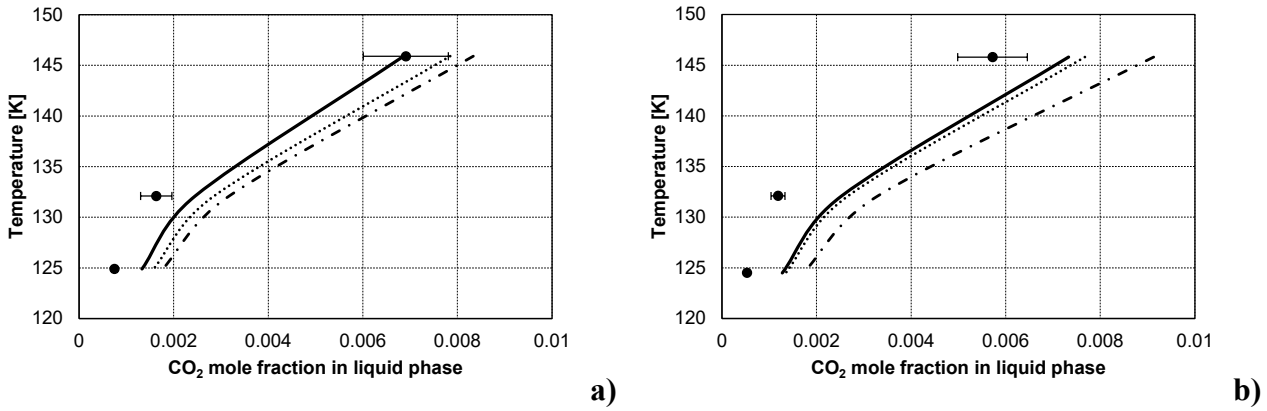

Figure 14. CO_2 mole fraction in the liquid phase at SLVE conditions for the CO_2-CH_4-N_2 system: comparison between the results obtained with the proposed algorithm (solid line), by simulation of RGibbs in Aspen Plus® V9.0[42] (dashed and dotted line), and by Riva and Stringari[14] (dotted line). Two mixtures are considered: a) Mixture 1: 2 mol.% CO_2, 58 mol.% CH_4, 40 mol.% N_2; b) Mixture 2: 2 mol.% CO_2, 79 mol.% CH_4, 19 mol.% N_2.

4.3 The CO_2-CH_4-N_2-O_2 system

Riva and Stringari[14] presented SLVE data for two mixtures consisting of CO_2, CH_4, N_2 and O_2, and applied the same calculation approach used for the ternary mixture without oxygen (described in the previous section) to SLVE calculations for these two quaternary mixtures. Such mixtures are characterized by the same content of CO_2 and CH_4 as the two ternary mixtures in which O_2 was not present, and the percentage of N_2 is consequently decreased in favour of O_2. The experimental data and the calculation results obtained with their approach, as well as with the two ones taken into account in this work, are illustrated in Figures 15-16.

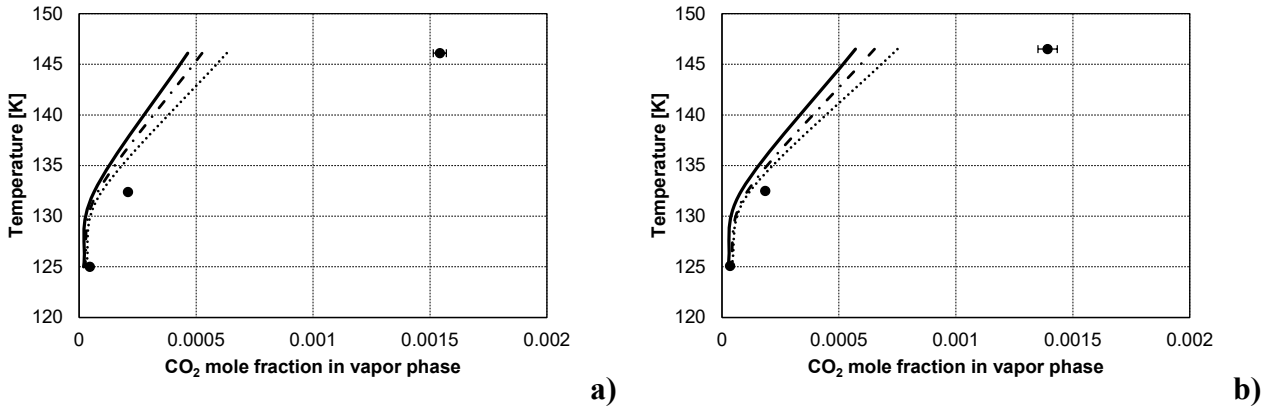

Figure 15. CO_2 mole fraction in the vapor phase at SLVE conditions for the CO_2-CH_4-N_2-O_2 system: comparison between the results obtained with the proposed algorithm (solid line), by simulation of RGibbs in Aspen Plus® V9.0[42] (dashed and dotted line), and by Riva and Stringari[14] (dotted line). Two mixtures are considered: a) Mixture 1: 2 mol.% CO_2, 58 mol.% CH_4, 31 mol.% N_2, 9 mol.% O_2; b) Mixture 2: 2 mol.% CO_2, 79 mol.% CH_4, 15 mol.% N_2, 4 mol.% O_2.

It is possible to notice that, according to the experimental values, the CO_2 mole fraction in the vapor phase at SLVE increases when some nitrogen is replaced by oxygen (Figure 15 *vs.* Figure 13), but this phenomenon is not correctly predicted by any of the three approaches. The availability of more experimental data for this quaternary mixture will certainly help to better understand the reason for these discrepancies.

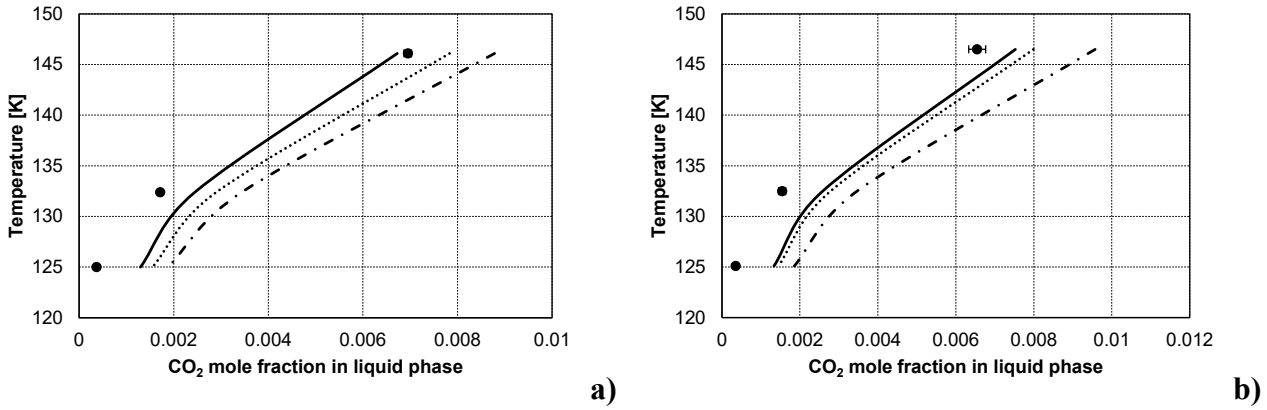

Figure 16. CO_2 mole fraction in the liquid phase at SLVE conditions for the CO_2-CH_4-N_2-O_2 system: comparison between the results obtained with the proposed algorithm (solid line), by simulation of RGibbs in Aspen Plus® V9.0[42] (dashed and dotted line), and by Riva and Stringari[14] (dotted line). Two mixtures are considered: a) Mixture 1: 2 mol.% CO_2, 58 mol.% CH_4, 31 mol.% N_2, 9 mol.% O_2; b) Mixture 2: 2 mol.% CO_2, 79 mol.% CH_4, 15 mol.% N_2, 4 mol.% O_2.

The mole fraction of CO_2 in the liquid phase is overestimated by the different approaches, as can be seen in Figure 16, with the exception of the point at the highest temperature in Figure 16a as for the results obtained with the proposed approach that performs better than the other two ones. This behavior may be explained considering that the parameters used by the thermodynamic models for the fluid phases (e.g., the binary interaction parameters, k_{ij}s, for the Peng Robinson EoS) are optimized for the vapor-liquid equilibrium at conditions different from the ones at which they are in equilibrium with solid CO_2. Though the three approaches make use of different thermodynamic models and are based on the implementation of different algorithms (Rachford-Rice method coupled to a phase stability analysis as for the proposed algorithm; Gibbs energy minimization as for the RGibbs tool; classical approach based on the isofugacity condition as for the approach adopted by Riva and Stringari[14]), they are consistent with each other. Therefore, as also stated by the authors presenting the experimental data for the quaternary mixture, "more experimental studies are suggested to provide a full description of the system behavior as a function of temperature, pressure, and nitrogen and/or oxygen mole fraction".[14]

5. Conclusions

This work deals with phase equilibria in the presence of solid CO_2 for mixtures of interest in the fields of natural gas purification and biogas/landfill gas upgrading. Experimental data for solid-vapor equilibria and solid-liquid-vapor equilibria available in the literature are first reviewed, reporting the type of measurements they refer to for the CO_2-CH_4 binary mixture, the CO_2-CH_4-N_2 ternary mixture and the CO_2-CH_4-N_2-O_2 quaternary mixture. Such data have been used for the validation of a thermodynamic calculation approach that allows coupling a phase stability analysis with isothermal-

isobaric flash computations in multiphase systems at given temperature, pressure and their global composition without knowing *a-priori* the number and the type of phases present at equilibrium. The algorithm can be applied to calculations of phase diagrams involving the liquid and vapor fluid phases and a solid phase, which consists of pure CO_2, and will be further developed in the future to account for the presence of more phases, so to allow the application to more complex systems, such as those that may exhibit a miscibility gap and lead to liquid-liquid equilibria at certain temperature and pressure conditions.

The proposed algorithm has turned out to satisfactorily predict the behavior of the mixtures taken into account, with an average absolute deviation not higher than 1.3 % when considering, for example, the calculation of CO_2 frost point temperature in the binary mixture with methane. In some cases, especially for the quaternary mixture, the results are in good agreement with those obtained with other approaches based on different models, but to a lesser extent with the few available experimental data. To better assess the reliability of the proposed algorithm, more experimental studies are needed to enrich the database, especially for multicomponent mixtures involving non-hydrocarbon compounds in addition to carbon dioxide and methane. Nitrogen and oxygen are two of them, which can be found in natural gas and in biogas/landfill gas. Since CO_2 has to be separated from these gases to produce a pipeline-quality gas or liquefied natural gas (LNG)/liquefied biomethane (bioLNG), and some processes for this purpose are operated at conditions where solid CO_2 may form, process engineers should know at which conditions the process has to be operated if the formation of dry ice has to be avoided. For this, the availability of more experimental data (e.g., at higher concentrations of nitrogen, which can reach 40 mol.%[5] and larger values in natural gas or associated gas, at concentrations of CO_2 higher than 20 mol% - the maximum value for which SVE and/or SLVE data are now available in the literature for the ternary and quaternary mixture taken into account in this work – and at pressures higher than 20 bar at which some CO_2 low-temperature/cryogenic separation processes are operated) could allow a better description of the system thermodynamic behavior as a function of temperature, pressure, and composition and could, consequently, allow a better process design.

Supporting Information

Details on: i) the experimental literature data used for validation of the proposed algorithm; ii) the properties of the components taken into account in this work and the theoretical background for the algorithm proposed for simultaneous multiphase flash and stability analysis calculations including solid CO_2.

References

(1) Babar, M.; Bustam, M.A.; Ali, A.; Maulud, A.S.; Shafiq, U.; Mukhtar, A.; Shah, S.N.; Maqsood, K.; Mellon, N.; Shariff, A.M., Thermodynamic data for cryogenic carbon dioxide capture from natural gas: a review. *Cryogenics* **2019,** 102, 85-104.

(2) Pellegrini, L.A.; Langè, S.; Baccanelli, M.; De Guido, G., Techno-Economic Analysis of LNG Production Using Cryogenic Vs Conventional Techniques for Natural Gas Purification. In *Offshore Mediterranean Conference and Exhibition*, Offshore Mediterranean Conference: Ravenna, Italy, 2015.

(3) Pellegrini, L.A.; De Guido, G.; Langé, S., Biogas to liquefied biomethane via cryogenic upgrading technologies. *Renewable Energy* **2017,** 124, 75-83.

(4) Pellegrini, L.A.; De Guido, G.; Langè, S.; Moioli, S.; Picutti, B.; Vergani, P.; Franzoni, G.; Brignoli, F., The Potential of a New Distillation Process for the Upgrading of Acid Gas. In *Abu Dhabi International Petroleum Exhibition & Conference (ADIPEC)*, Society of Petroleum Engineers: Abu Dhabi, UAE, 2016.

(5) De Guido, G.; Messinetti, F.; Spatolisano, E., Cryogenic Nitrogen Rejection Schemes: Analysis of Their Tolerance to CO_2. *Industrial & Engineering Chemistry Research* **2019,** 58(37), 17475-17488.

(6) Pikaar, M.J. A study of phase equilibria in hydrocarbon-CO_2 systems. Ph.D. Thesis, Imperial College of Science and Technology, London, 1959.

(7) Le, T.T.; Trebble, M.A., Measurement of carbon dioxide freezing in mixtures of methane, ethane, and nitrogen in the solid− vapor equilibrium region. *Journal of Chemical & Engineering Data* **2007,** 52(3), 683-686.

(8) Agrawal, G.; Laverman, R., Phase behavior of the methane-carbon dioxide system in the solid-vapor region. In *Advances in Cryogenic Engineering*, Springer: 1995; pp 327-338.

(9) Zhang, L.; Burgass, R.; Chapoy, A.; Tohidi, B.; Solbraa, E., Measurement and Modeling of CO_2 Frost Points in the CO_2–Methane Systems. *Journal of Chemical & Engineering Data* **2011,** 56(6), 2971-2975.

(10) De Guido, G.; Fogli, M.R.; Pellegrini, L.A., Effect of Heavy Hydrocarbons on CO_2 Removal from Natural Gas by Low-Temperature Distillation. *Industrial & Engineering Chemistry Research* **2018,** 57(21), 7245-7256.

(11) Xiong, X.; Lin, W.; Jia, R.; Song, Y.; Gu, A., Measurement and calculation of CO_2 frost points in CH_4+ CO_2/CH_4+ CO_2+ N_2/CH_4+ CO_2+ C_2H_6 mixtures at low temperatures. *Journal of Chemical & Engineering Data* **2015,** 60(11), 3077-3086.

(12) Shen, T.; Gao, T.; Lin, W.; Gu, A., Determination of CO_2 solubility in saturated liquid CH_4+ N_2 and CH_4+ C_2H_6 mixtures above atmospheric pressure. *Journal of Chemical & Engineering Data* **2012,** 57(8), 2296-2303.

(13) Gao, T.; Shen, T.; Lin, W.; Gu, A.; Ju, Y., Experimental determination of CO_2 solubility in liquid CH_4/N_2 mixtures at cryogenic temperatures. *Industrial & Engineering Chemistry Research* **2012,** 51(27), 9403-9408.

(14) Riva, M.; Stringari, P., Experimental study of the influence of nitrogen and oxygen on the solubility of solid carbon dioxide in liquid and vapor methane at low temperature. *Industrial & Engineering Chemistry Research* **2018,** 57(11), 4124-4131.

(15) Donnelly, H.G.; Katz, D.L., Phase equilibria in the carbon dioxide–methane system. *Industrial & Engineering Chemistry* **1954,** 46(3), 511-517.

(16) Sterner, C., Phase equilibria in the CO_2-methane systems. In *Advances in Cryogenic Engineering*, Springer: 1961; pp 467-474.

(17) Davis, J.; Rodewald, N.; Kurata, F., Solid-liquid-vapor phase behavior of the methane-carbon dioxide system. *AIChE Journal* **1962,** 8(4), 537-539.

(18) Im, K.U.; Kurata, F., Phase equilibrium of carbon dioxide and light paraffins in presence of solid carbon dioxide. *Journal of Chemical & Engineering Data* **1971,** 16(3), 295-299.

(19) Brewer, J.; Kurata, F., Freezing points of binary mixtures of methane. *AIChE Journal* **1958,** 4(3), 317-318.

(20) Haufe, S.; Tieize, G.; Muller, H., Solubility of solid carbon-dioxide in a mixture of methane and nitrogen. *Chemische Technik* **1972,** 24(10), 619.

(21) De Guido, G.; Langè, S.; Moioli, S.; Pellegrini, L.A., Thermodynamic method for the prediction of solid CO_2 formation from multicomponent mixtures. *Process Safety and Environmental Protection* **2014,** 92(1), 70-79.

(22) Gupta, A.K. Steady state simulation of chemical processes. Ph.D. Thesis, University of Calgary, Calgary, 1990.

(23) Gautam, R.; Seider, W.D., Computation of phase and chemical equilibrium: Part I. Local and constrained minima in Gibbs free energy. *AIChE Journal* **1979,** 25(6), 991-999.

(24) Michelsen, M.L., The isothermal flash problem. Part I. Stability. *Fluid Phase Equilibria* **1982,** 9(1), 1-19.

(25) Michelsen, M.L., The isothermal flash problem. Part II. Phase-split calculation. *Fluid Phase Equilibria* **1982,** 9(1), 21-40.

(26) Michelsen, M.L., Multiphase isenthalpic and isentropic flash algorithms. *Fluid Phase Equilibria* **1987,** 33(1-2), 13-27.

(27) Wu, J.-S.; Bishnoi, P., An algorithm for three-phase equilibrium calculations. *Computers & Chemical Engineering* **1986,** 10(3), 269-276.
(28) Castier, M.; Rasmussen, P.; Fredenslund, A., Calculation of simultaneous chemical and phase equilibria in nonideal systems. *Chemical Engineering Science* **1989,** 44(2), 237-248.
(29) Gupta, A.K.; Bishnoi, P.R.; Kalogerakis, N., Simultaneous multiphase isothermal/isenthalpic flash and stability calculations for reacting/non-reacting systems. *Gas Separation & Purification* **1990,** 4(4), 215-222.
(30) Gupta, A.K.; Bishnoi, P.R.; Kalogerakis, N., A method for the simultaneous phase equilibria and stability calculations for multiphase reacting and non-reacting systems. *Fluid Phase Equilibria* **1991,** 63(1-2), 65-89.
(31) Ballard, A.; Sloan Jr, E., The next generation of hydrate prediction: Part III. Gibbs energy minimization formalism. *Fluid Phase Equilibria* **2004,** 218(1), 15-31.
(32) Segtovich, I.S.V.; Barreto Jr, A.G.; Tavares, F.W., Simultaneous multiphase flash and stability analysis calculations including hydrates. *Fluid Phase Equilibria* **2016,** 413, 196-208.
(33) Tang, L.; Li, C.; Lim, S., Solid–Liquid–Vapor Equilibrium Model Applied for a CH_4–CO_2 Binary Mixture. *Industrial & Engineering Chemistry Research* **2019,** 58(39), 18355-18366.
(34) Jäger, A.; Span, R., Equation of state for solid carbon dioxide based on the Gibbs free energy. *Journal of Chemical & Engineering Data* **2012,** 57(2), 590-597.
(35) De Guido, G.; Pellegrini, L., Application of Conventional and Novel Low-temperature CO_2 Removal Processes to Lng Production at Different CO_2 Concentrations in Natural Gas. *Chemical Engineering Transactions* **2019,** 74, 853-858.
(36) Qyyum, M.A.; Haider, J.; Qadeer, K.; Valentina, V.; Khan, A.; Yasin, M.; Aslam, M.; De Guido, G.; Pellegrini, L.A.; Lee, M., Biogas to liquefied biomethane: Assessment of 3P's–Production, processing, and prospects. *Renewable and Sustainable Energy Reviews* **2020**, 109561.
(37) Ballard, A.L. A non-ideal hydrate solid solution model for a multi-phase equilibria program. Ph.D. Thesis, Colorado School of Mines, 2002.
(38) Peng, D.-Y.; Robinson, D.B., A new two-constant equation of state. *Industrial & Engineering Chemistry Fundamentals* **1976,** 15(1), 59-64.
(39) Jensen, M.J.; Russell, C.S.; Bergeson, D.; Hoeger, C.D.; Frankman, D.J.; Bence, C.S.; Baxter, L.L., Prediction and validation of external cooling loop cryogenic carbon capture (CCC-ECL) for full-scale coal-fired power plant retrofit. *International Journal of Greenhouse Gas Control* **2015,** 42, 200-212.
(40) Friend, D.G.; Ely, J.F.; Ingham, H., Thermophysical properties of methane. *Journal of Physical and Chemical Reference Data* **1989,** 18(2), 583-638.

(41) Pellegrini, L.A.; De Guido, G.; Ingrosso, S. In *Thermodynamic Framework for Cryogenic Carbon Capture*, 30th European Symposium on Computer Aided Process Engineering (ESCAPE30), Milan, Italy, May 24-27, 2020, 2020; Elsevier B.V: Milan, Italy, 2020.
(42) AspenTech *Aspen Plus®,Burlington (MA), United States*; AspenTech: Burlington (MA), United States, 2016.

For Table of Contents Only